Chemistry–A European Journal
Review
doi.org/10.1002/chem.202402754
Chemistry Europe
European Chemical Societies Publishing
www.chemeurj.org

Recent Advances in Electrolytes for Magnesium Batteries: Bridging the gap between Chemistry and Electrochemistry

Sibylle Riedel,*[a] Liping Wang,[b] Maximilian Fichtner,[a, c] and Zhirong Zhao-Karger*[a, c]

Rechargeable magnesium batteries (RMBs) have the potential to provide a sustainable and long-term solution for large-scale energy storage due to high theoretical capacity of magnesium (Mg) metal as an anode, its competitive redox potential (Mg/Mg^{2+}:−2.37 V vs. SHE) and high natural abundance. To develop viable magnesium batteries with high energy density, the electrolytes must meet a range of requirements: high ionic conductivity, wide electrochemical potential window, chemical compatibility with electrode materials and other battery components, favourable electrode-electrolyte interfacial properties and cost-effective synthesis. In recent years, significant progress in electrolyte development has been made. Herein, a comprehensive overview of these advancements is presented. Beginning with the early developments, we particularly focus on the chemical aspects of the electrolytes and their correlations with electrochemical properties. We also highlight the design of new anions for practical electrolytes, the use of electrolyte additives to optimize anode-electrolyte interfaces and the progress in polymer electrolytes.

1. Introduction

With society's increasing electrification, the expanded use of energy storage systems has become essential, especially as a complimentary option to the current lithium-based technology. In the quest for environmentally friendly, safe, and cost-effective alternatives, magnesium-based systems emerge as a promising solution. Magnesium offers a higher volumetric capacity than lithium (Mg: 3833 mAh cm^{-3} vs. Li: 2062 mAh cm^{-3}) and is considerably more abundant in nature. The high abundance, combined with the potential to reach comparable or higher capacities, could lead to significant cost reductions of the battery production. A major reason for achieving high volumetric energy densities is the use of with metallic Mg anodes. However, discovering an electrolyte that can facilitate reversible Mg plating/stripping at the anode, supports reversible intercalation/deintercalation in high-voltage cathodes, and demonstrates long-term stability remains a significant scientific and technical challenge. Overcoming this challenge is crucial for advancing magnesium battery technology.[1–4] The electrolyte development for RMBs has shown promising progress in the past twenty years.[3–8] However, this area of research is still in its early stages. There are still many open questions, such as understanding the electrode/electrolyte interfaces in different electrolyte systems and exploring the chemical and electrochemical compatibility. Therefore, additional research and investigations are necessary to gain a comprehensive understanding of the challenges involved and to enable a market introduction of Mg batteries.

In general, the electrolyte composition must satisfy the multiple requirements: weak cation-anion pairing offering sufficient ionic conductivity, electrochemical stability within the battery voltage range, chemical compatibility with the electrodes to prevent parasitic reactions in the batteries; formation of ion-conducting stable electrode-electrolyte interfaces; non-corrosiveness to current collectors and battery housing components. Additionally, ease of synthesis, low-cost and low toxicity are desirable features. To fulfil these critical criteria, various approaches have been explored, including optimizing the traditional Grignard-based complex electrolytes, designing new anions, identifying additives to form suitable anode/electrolyte interfaces, and designing of polymer electrolytes. These approaches will be discussed in the following chapters.

1.1. Overview of Various Types of Magnesium Electrolytes

The first study of magnesium batteries dates back more than 30 years.[9] Subsequently, Aurbach *et al.* pioneered the development of the first rechargeable magnesium battery prototype utilizing a Grignard-based electrolyte solution.[10] Building upon this milestone, further electrolyte compositions based on Grignard or complex salts (Lewis base-acid combinations) with chlorides ($MgCl_2$, $AlCl_3$) were developed over the next few years.[11–16] All these compositions share two common characteristics: a narrow voltage range and high corrosiveness due to the chlorides.

[a] S. Riedel, M. Fichtner, Z. Zhao-Karger
Helmholtz Institute Ulm (HIU), Electrochemical Energy Storage, Helmholtzstrasse 11, 89081 Ulm, Germany
E-mail: zhirong.zhao-karger@kit.edu
sibylle.riedel@partner.kit.edu
[b] L. Wang
Institute for Organic Chemistry II and Advanced Materials, Ulm University, Albert-Einstein-Allee 11, 89081 Ulm, Germany
[c] M. Fichtner, Z. Zhao-Karger
Institute of Nanotechnology (INT), Karlsruhe Institute of Technology (KIT), Hermann-von-Helmholtz Platz 1, 76344 Eggenstein-Leopoldshafen, Germany

For these reasons, the development of Mg electrolytes shifted towards chloride-free single salts in order to obtain high-voltage RMBs with extended lifetimes. New anions were developed for this purpose as well, with borate-based anions emerging as the most promising representatives (*e.g.* $[B(hfip)_4]^-$, $(CB_{11}H_{12})^-$).[17,18] Commercial single salts, such as $Mg(TFSI)_2$ and $Mg(OTf)_2$, were also subjected to further tests, but in most cases, the addition of $MgCl_2$ was still necessary to maintain a satisfactory performance. As a result, further studies were initiated on finding other additives which showed similar positive effects as $MgCl_2$ but without the associated negative influences.[19–23]

Recently, developments have extended to magnesium polymer electrolytes, which are in particular supposed to improve the long-term stability of the magnesium-sulfur (Mg–S) battery chemistry and the safety of the cells.[24–28] A chronological overview and examples of the developments of various electrolyte systems are shown in Figure 1.

2. Early developments of $MgCl^+$ based complex electrolytes

Gregory *et al.* began the first experiments on Mg deposition and dissolution in 1990. They used various organo magnesium chlorides mixed with $AlCl_3$ in THF as a solvent and were able to demonstrate successful Mg electrodeposition.[9] Ten years later the first rechargeable magnesium battery prototype was demonstrated with an electrolyte prepared from the combination of Bu_2Mg and $EtAlCl_2$ in THF, Mg metal anode, and Chevrel phase as cathode.[10] However, this electrolyte system showed a rather low oxidation stability (~2.5 V). Based on these approaches, the development of the so-called APC ("all phenyl complex") electrolyte improved the stability to approx. 3.5 V by using PhMgCl and $AlCl_3$ as the precursors.[16,29]

All successful traditional electrolyte systems thus far are nucleophilic, but non-nucleophilic electrolytes are necessary for a wider application with different cathode materials, such as sulfur. For this purpose, Kim *et al.* created a non-nucleophilic complex electrolyte system prepared by mixing HMDSMgCl and $AlCl_3$ in THF, where they isolated the crystals and determined the structure by single-crystal X-ray diffraction [$(Mg_2(\mu\text{-}Cl)_3{\cdot}6THF)$ $(HMDS_nAlCl_3)$].[30] The isolated complex salt was redissolved and used as electrolyte, showing good anodic stability (~3.2 V vs. Pt). Further, the compatibility of this type of electrolyte with the electrophilic sulfur cathode was demonstrated. Zhao-Karger *et al.* applied a simplified approach for the HMDS based non-nucleophilic electrolytes.[31] In a one-pot reaction magnesium-bis(hexamethyl-disilazide) $(Mg(HMDS)_2)$ and $AlCl_3$ were mixed in a ratio of 1:2 in ethereal solvents, and the electrolyte is generated in solution *in situ*. By using THF as solvent, they were able to present results comparable to Kim *et al.*[30] Additionally, they prepared the electrolyte solution with different glymes with and without an ionic liquid, and with additional $MgCl_2$. They compared the results and showed the compatibility of their system with a sulfur cathode.[32] The application of higher glymes as solvent improved the anodic stability (up to 3.7 V vs. Pt).

Dr. Sibylle Riedel is a postdoctoral researcher for advanced battery materials at the Helmholtz-Institute Ulm for Electrochemical Energy Storage (HIU) and Karlsruhe Institute of Technology (KIT) funded by the German Cluster of Excellence POLiS ("Energy Storage Beyond Lithium"). She received her Ph.D. in organic chemistry at the University of Tübingen and joined HIU and KIT 2021 with a focus on post-lithium batteries, specifically magnesium- and calcium-based systems. Her project involves the development of novel electrolytes and organic cathodes.

Dr. Liping Wang is currently a research scientist at Ulm University (UUlm). She received Ph.D. in physical chemistry from the University of Chinese Academy of Sciences in 2019, during which she spent one year as a visiting scholar at the HIU. From 2019 to 2022, she worked as a research scientist at KIT. Subsequently, she joined UUlm funded by the German Cluster of Excellence POLiS, where her research focuses on post-lithium batteries, specifically magnesium- and calcium-based systems. Her project involves the development of novel electrolytes and sulfur cathodes.

Dr. Zhirong Zhao-Karger is a research group leader for advanced battery materials at the Institute of Nanotechnology (INT) of the KIT. She received her Ph.D. in organic chemistry at the University Hannover, Germany. After the postdoctoral research at the Catalysis Research Laboratory of the University of Heidelberg, she joined the INT as a research scientist in 2008 and has been working in the field of electrochemical energy storage since 2013 with a focus on post-lithium batteries, such as magnesium and calcium-based systems.

Prof. Dr. Maximilian Fichtner is chemist, director at HIU, professor for Solid State Chemistry at UUlm, head of the department "Energy Storage Systems" at INT of KIT, scientific director of CELEST (Center for Electrochemical Energy Storage Ulm-Karlsruhe), spokesperson of the POLiS-cluster and a core team member of a new European flagship on battery research ("BATTERY2030+"). His research interests are raw materials, sustainability issues, new principles for energy storage and synthesis and investigation of related materials. He is (co)-author of approx. 450 publications, conference- and book contributions, 20 patents and editor of a book on magnesium batteries (h index: 70).

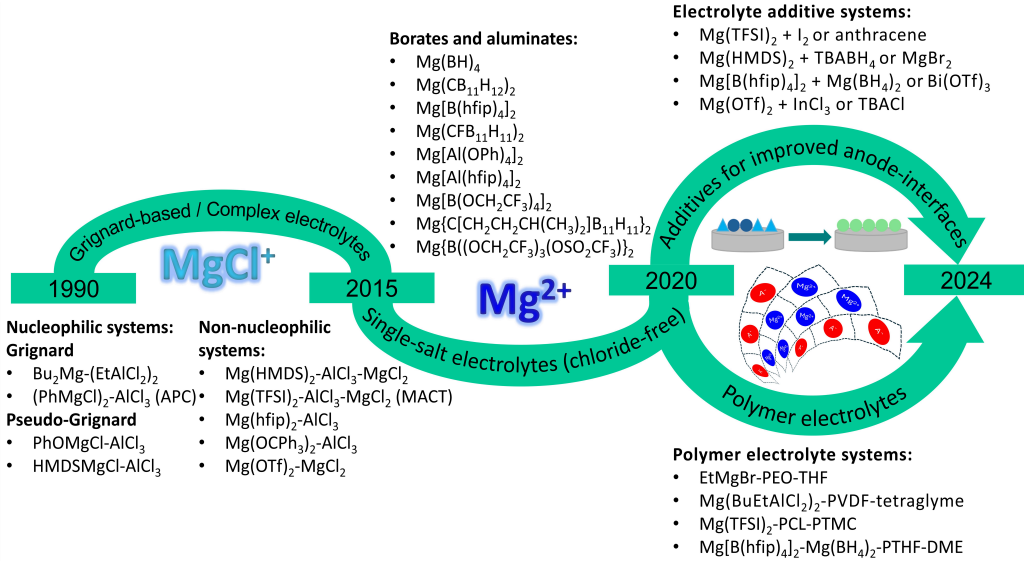

Figure 1. Overview of various representative electrolyte systems in the development stages: Grignard-based systems → complex electrolytes → single salt electrolytes → optimization with additives and development of polymer electrolytes.

Wang *et al.* presented a non-Grignard type electrolyte based on 2-*tert*-butyl-4-methyl-phenolate (BMP).[33] They prepared a solution of BMP magnesium chloride (BMPMC; [(2-$(CH_3)_3C$)(4-CH_3)C_6H_3OMgCl]) as Lewis base in THF, mixed it with $AlCl_3$ as Lewis acid, dissolved in THF and used the resulting composition as electrolyte. This electrolyte solution exhibited good ionic conductivity (2.56 mS cm^{-1}), reversible stripping/plating, high Coulombic efficiency (99%) and good compatibility with a Chevrel phase cathode, but suffered in anodic stability (~2.6 V vs. Pt). Furthermore, they denoted the mixture as air insensitive, which is a benefit for practical applications. Furthermore, Zhao-Karger *et al.* prepared a pseudo-Grignard electrolyte ([Mg_2Cl_3][$PhOAlCl_3$]), by mixing $PhOAlCl_2$ and $MgCl_2$ in diglyme.[34] They presented good anodic stability (3.4 V vs. Pt) and ionic conductivity (2.6 mS cm^{-1}). Moreover, while this electrolyte is deemed to be air insensitive, it suffers from a relatively low Coulombic efficiency (85%). As the $AlCl_3$-based systems showed promising results, this led to further combinations with this Lewis acid. Different magnesium salts like alkoxylates ($Mg(hfip)_2$, $Mg(OCPh_3)_2$, $Mg(PFTB)_2$, (hfip = OC-(H)$(CF_3)_2$; PFTB = $OC(CF_3)_3$), magnesium borate trichloride ($B(OMgCl)_3$) and $Mg(TFSI)_2$ were complexed with $AlCl_3$ and tested.[15,35–38] All these systems have the very corrosive Lewis acid $AlCl_3$ in common. For this reason, attempts were made in further developments to avoid its use.

Xiao *et al.* combined $Mg(PFTB)_2$ with $MgCl_2$, which led to high Coulombic efficiency (99.7%) and an anodic stability > 3.0 V.[39] Pan *et al.* complexed (DTBP)MgCl (DTBP = 2,6-di-*tert*-butylphenolate; {[2,6-$(CH_3)_3C]_2C_6H_3O$}) with $MgCl_2$ in THF and reached high Coulombic efficiency (CE = ~100%). Unfortunately, the anodic stability was quite low (~2.3 V vs. Pt).[40] Combining $Mg(HMDS)_2$ and $MgCl_2$ led to better results (CE = ~99%, anodic stability = ~2.8 V vs. Pt).[41] Merrill *et al.* compared the performance of complexing $Mg(HMDS)_2$ with $AlCl_3$ or $MgCl_2$. Voltage window-wise $AlCl_3$ is the winner (~2.8 V ($MgCl_2$) vs. ~3.2 V ($AlCl_3$)), but regarding the efficiency $MgCl_2$ performed better (CE_{MgCl2} = ~99%, CE_{AlCl3} = ~92%).[14] Going back to Grignard reagents, interestingly, when PhMgCl is complexed with $MgCl_2$, instead of $AlCl_3$ the oxidation stability was strongly improved (2.8 V to 3.8 V vs. Pt). Further, introducing a chloride-based ionic liquid led to a slight improvement in anodic stability (1.8 to 2.8 V vs. Ni).[42,43] Magnesium triflate ($Mg(OTf)_2$), as a commercially available salt, was studied by Nguyen *et al.* The combination of $Mg(OTf)_2$ and $MgCl_2$ led to good anodic stability (~3.0 V vs. Pt) and Coulombic efficiency (> 99%).[44] Most of these discussed electrolytes were tested in half cells using Chevrel phase cathodes and Mg metal anodes. Furthermore, the combination of Mg anode with sulfur-based cathodes, using non-nucleophilic complex electrolytes, was demonstrated.

Ren *et al.* combined magnesium bis-(diisopropyl)amide (MBA; $Mg[((CH_3)_2CH)_2N]_2$) with AlF_3, the ionic liquid $PP_{14}TFSI$ (1-butyl-1-methylpiperidinium bis(trifluoromethyl-sulfonyl)imide) and LiTFSI as additive to get a chloride-free alternative system.[45] The system showed reversible Mg plating/stripping, but with low anodic stability (~2.2 V vs. SS). Another approach was applied by Ilic *et al.* They prepared a mixture of $Mg(TFSI)_2$ and $Mg(OTf)_2$, which demonstrated promising plating/stripping behaviour and Coulombic efficiency (~92%) in a chloride-free system.[46] Yang *et al.* recently presented the combination of $Mg(OTf)_2$ and 1-chloropropane. Reversible plating/stripping, high Coulombic efficiency (99.79%) and good anodic stability (3.06 V vs. Pt) were reached.[13] However, when using 1-chloropropane, it should be considered that it is a Grignard precursor, which can chemically react with the magnesium metal anode, leading to the formation of propyl magnesium chloride and the Schlenk equilibrium can lead to $MgCl_2$. The presence of chloride ions is also reflected in an only moderate anodic stability (~3.0 V vs. Pt). Furthermore, they describe a chloride-rich surface layer at the electrode after cycling.

Table 1. List of complex Mg electrolytes and a summary of their electrochemical properties.

Lewis base- acid combinations	Solvent	Ionic conductivity at rt [mS cm^{-1}]	Anodic stability [V]	Efficiency [%]	Ref.
Bu_2Mg-$(EtAlCl_2)_2$	THF	several	~2.5 vs. Pt	~100	[10]
$(PhMgCl)_2$-$AlCl_3$ (APC)	THF	2–5	~3.5 vs. Pt	~100	[29]
HMDSMgCl-$AlCl_3$	THF	–	~3.2 vs. Pt	~100	[30]
{2-[$(CH_3)_3C$](4-CH_3) C_6H_3O}MgCl-$AlCl_3$	THF	2.56	~2.6 vs. Pt	99	[33]
$Mg(HMDS)_2$-$AlCl_3$	diglyme	1.70	3.9 vs. Pt	99	[31]
$PhOAlCl_2$-$MgCl_2$	diglyme	2.6	3.4 vs. Pt	85	[34]
$Mg(hfip)_2$-$AlCl_3$	DME	4.77	~3.0 vs. Pt	~100	[35]
$Mg(OCPh_3)_2$-$AlCl_3$	THF	–	~2.8 vs. Pt	~80	[15]
$(Mg[OC(CF_3)_3]_2)$-$AlCl_3$-$MgCl_2$	DME	–	~3.8 vs. Mo	99.5	[36]
$Mg[OC(CF_3)_3]_2$-$MgCl_2$	THF	–	> 3.0 vs. Pt	99.7	[39]
$B(OMgCl)_3$-$AlCl_3$	triglyme	2.15	~3.0 vs. Pt	~64	[37]
$Mg(TFSI)_2$-$AlCl_3$-$MgCl_2$ (MACT)	DME	6.82	~3.2 vs. Pt	~96	[38]
{[2,6-$(CH_3)_3C]_2C_6H_3O$}MgCl-$MgCl_2$	THF	0.66	~2.3 vs. Pt	~100	[40]
$Mg(HMDS)_2$-$MgCl_2$	THF	0.5	~2.8 vs. Pt	~99	[14,41]
$Mg(HMDS)_2$-$AlCl_3$-$MgCl_2$	diglyme/tetraglyme	–	~3.3/~3.7 vs. Pt	-	[32]
$Mg(HMDS)_2$-$AlCl_3$-$MgCl_2$	$PP_{14}TFSI$/ tetraglyme-$PP_{14}TFSI$	–	~3.3/~3.7 vs. Pt	-	[32]
$Mg(HMDS)_2$-$AlCl_3$	THF	–	~3.2 vs. Pt	~92	[14]
PhMgCl-$MgCl_2$	THF	0.79	~3.8 vs. Pt	~95	[42]
PhMgCl-AMPyrrCl	THF	0.23–0.60	~2.8 vs. Ni	~100	[43]
$Mg(OTf)_2$-$MgCl_2$	DME	0.34–0.53	~3.0 vs. Pt	99.1	[44]
$Mg[OC(CF_3)_3]_2$-$AlCl_3$	THF	–	~3.0 vs. SS	~99	[47]
$Mg[OC(CF_3)_3]_2$-$AlCl_3$	DME	–	~2.5 vs. SS	~99	[47]
$Mg[((CH_3)_2CH)_2N]_2$-AlF_3-$PP_{14}TFSI$-LiTFSI	THF	3.78	2.2 vs. SS	~90	[45]
$Mg(TFSI)_2$-$Mg(OTf)_2$	diglyme	–	1.35 vs, Ag/Ag+	~92	[46]
$Mg(OTf)_2$-1-chloropropane	DME	–	3.06 vs. Pt	99.79	[13]
$[Mg_2Cl_3(THF)_6][1$-$(1,7$-$C_2B_{10}H_{11})_2MgCl(THF)]$	THF	0.6	3.2 vs. Al	98.2	[48]

All these results indicate that chloride plays an important role in reaching high efficiencies, especially for the commercially available magnesium salts. That's why nearly all the systems discussed contain significant amounts of chloride ions, which are corrosive to conventional current collectors and showed a short battery life (< 100 cycles) and a limited voltage range (< 4.0 V).

To overcome these challenges, electrolyte systems without chloride ions are required. The properties of the discussed electrolytes are summarized in Table 1 and obtained single crystal structures of some examples are shown in Figure 2.

2.1. Properties of Complex Electrolytes

Complex electrolytes have characteristic chemical and electrochemical properties that we would like to explain them in more detail. The synthesis of these electrolytes is relatively easy. Generally, they are prepared by mixing a Lewis base with a Lewis acid. However, it has been revealed that the composition of such electrolytes is rather complicated, containing different cation and anion species.[9] Taking Grignard based electrolytes as an example, the Schlenk equilibrium will establish and transmetalations will take place, leading to different species in the electrolyte solutions (Scheme 1). In these electrolyte systems $Mg_2Cl_3^+$ and $MgCl^+$ complex cations are the redox-active species for Mg deposition.

Additionally, it has been revealed that the anion species in the electrolyte may induce parasitic reactions in the battery system.[29,49] Furthermore, chloride ions are corrosive to metallic collectors and other cell components and could lead to detrimental side reactions. The early electrolyte systems, based on Grignard reagents are nucleophilic and cannot be combined with electrophilic cathode materials (*e.g.*: sulfur, quinone type

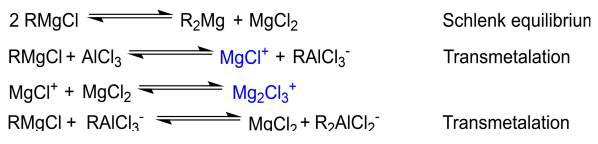

Scheme 1. Possible reactions within the electrolyte.

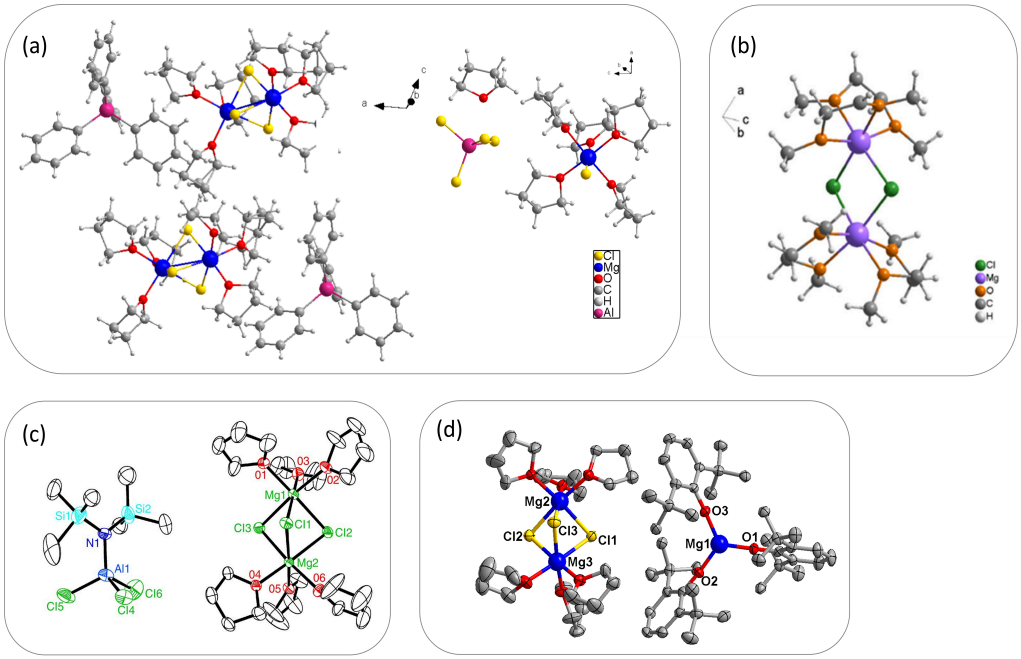

Figure 2. Single crystal structures: (a) APC-electrolyte: Precipitated from THF solutions of: left: 0.4 M $AlCl_3$ + 0.8 M PhMgCl, right: 0.25 M $AlCl_3$ + 0.125 M PhMgCl, by Pour *et al.* (Created in Diamond 4.0 using published data).[49]; (b) Cation of the $Mg(TFSI)_2$-$AlCl_3$-$MgCl_2$/DME electrolyte by Yang *et al.* Reproduced with permission.,[38] Copyright © 2021, American Chemical Society (c) $[Mg_2Cl_3$-6THF][HMDSAlCl$_3$] presented by Kim *et al.* Reproduced with permission.,[30] Springer Nature, Copyright © 2011, H. S. Kim, T. S. Arthur, G. D. Allred, J. Zajicek, J. G. Newman, A. E. Rodnyansky, A. G. Oliver, W. C. Boggess, J. Muldoon; (d) ($C_{14}H_{21}O$)MgCl-$MgCl_2$/DME obtained by Pan *et al.* (Created in Diamond 4.0 using published data).[50]

organic materials). The pseudo-Grignard based combinations showed less nucleophilicity, but only the later developed Lewis base-acid combinations with *e.g.*: $Mg(HMDS)_2$ or $Mg(TFSI)_2$ with $AlCl_3$ or $MgCl_2$ are non-nucleophilic and could be used for a broader range of cathode materials. However, Dong *et al.* proved that $MgCl^+$ is the actual charge carrier species rather than divalent Mg^{2+} in such complex electrolyte systems.[51] They compared the storage mechanisms of a $Mg(HMDS)_2$-$MgCl_2$ mixture and a single salt electrolyte ($Mg(CB_{11}H_{12})_2$), which will be discussed in the next chapter. As dominant shuttling species $MgCl^+$ is stored in the cathode instead of Mg^{2+}. However, the anode only stores Mg, the electrolyte must also serve as a Cl^- reservoir, and the amount of Cl^- in the electrolyte must be at least equal to the capacity of the cathode. The group compared the working mechanisms of 14PAQ–Mg cells (14PAQ: 1,4-poly anthraquinone) using the different types of electrolytes (Figure 3). With their experiments they were able to show, that about 1 order of magnitude more $MgCl^+$-electrolyte is necessary to reach the same capacity as when using Mg^{2+}-electrolyte. This leads to a lower energy density at cell level and demonstrates another advantage of single salt electrolytes, irrespective of corrosivity and nucleophilicity.

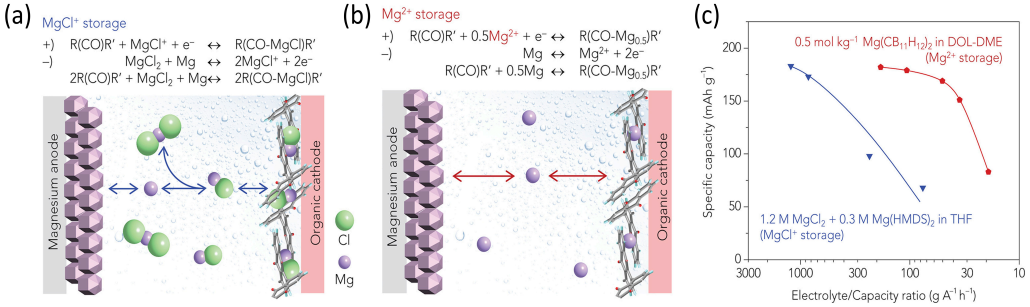

Figure 3. (a and b) Reaction schemes and schematic representation of the working mechanism of organic cathodes in (a) chloride-containing and (b) chloride-free electrolytes.; (c) Comparison of 14PAQ–Mg cells in electrolytes containing $MgCl^+$ and Mg^{2+} under lean electrolyte conditions as a function of the electrolyte:capacity (E:C) ratio. "E" represents the mass of electrolyte used in a cell, and "C" is the designed capacity based on a specific capacity of 193 mAh g^{-1} for 14PAQ. Reproduced with permission,[51] Copyright © 2018 Elsevier Inc.

3. Designing New Anions Towards Advanced Single Salt Electrolytes

3.1. Boron-Based Mg Salts

Mohtadi *et al.* initially investigated $Mg(BH_4)_2$-based electrolyte systems in different ether-based solvents. This electrolyte demonstrates reversible Mg plating and stripping in absence of chloride ions, but the systems suffer from low anodic stability (~1.7 V vs. Pt) and low Coulombic efficiency (67% in DME).[52] However, this approach can be regarded as the starting point for the development and evaluation of various boron-based magnesium salts.

3.1.1. Carboranes as Anions

Carter *et al.* synthesized the *closo*-borane magnesium dodecahydrododecaborate ($MgB_{12}H_{12}$) and attempted to investigate the electrolytic properties.[48] Unfortunately, it is insoluble in ethereal solvents. For a proof of concept of using boron clusters as stable anions, a carboranyl magnesium chloride (1-(1,7-$C_2B_{10}H_{11})_2MgCl$) was synthesized by reacting *m*-carborane with isopropyl magnesium chloride in THF under reflux and tested. The electrolyte solution in THF showed reversible Mg plating/stripping, high Coulombic efficiency (98.2%) and good anodic stability (~3.2 V vs. Pt).[48] This type of electrolyte is an analogue to the Grignard-based electrolytes, where $[Mg_2Cl_3]^+/MgCl^+$ complex cation is the redox active species. Further, Tutusaus *et al.* synthesized the magnesium monocarborane salt ($Mg(CB_{11}H_{12})_2$) and evaluated its suitability as electrolyte.[18] With a 0.75 M electrolyte solution in tetraglyme, they demonstrated reversible plating/stripping, high Coulombic efficiency (>90%) and high anodic stability (~3.8 V vs. Al). Moreover, they showed the utilization of this electrolyte in rechargeable magnesium batteries with Chevrel phase and α-MnO_2 as cathodes, respectively. Dong *et al.* demonstrated the feasibility of this type of electrolytes with an organic cathode, as this electrolyte is non-nucleophilic as well as non-corrosive.[53] In 2018 Hahn *et al.* carried out investigations in optimizing the $[CB_{11}H_{12}]^-$-anion. Replacing the C–H-group to a C–F should increase the anodic stability and further weaken the ionic attraction. With different calculations and initial electrochemical tests, they demonstrated the validity of this concept (CE = ~94% to 96%; anodic stability = ~3.8 V to >4 V).[54]

Recently, Tomich *et al.* published another approach in optimizing the boron cluster anion. They replaced the hydrogen at the carbon with alkylgroups. The $Mg\{C[CH_2CH_2CH(CH_3)_2]B_{11}H_{11}\}_2$ salt, dissolved in DME, showed higher solubility, conductivity (2.9 mS cm^{-1} to 7.3 mS cm^{-1}) and anodic stability (3.8 V to 4.2 V) compared to the simple salt $Mg(CB_{11}H_{12})_2$ in tetraglyme. However, when combining this electrolyte with a Chevrel Phase cathode in a full cell, the capacity decreased compared to the simple salt (40 mAh g^{-1} vs. 80 mAh g^{-1}).[55] Overall, this type of magnesium electrolytes shows promising performance, but the broader application suffers from the complicated and expensive synthetic pathways. As shown in Scheme 2 the boron clusters are synthesized starting from expensive precursors like $Ag(CB_{11}H_{12})$, $(HNMe_3)(CB_{11}H_{12})$ or $Cs(CB_{11}H_{12})$ (Me = CH_3). The high price is due to the time-consuming and complex synthesis and refining process.[18,54–60]

3.1.2. Borates as Anions

As mentioned before, a high anodic stability is one of the key factors for a suitable electrolyte. One approach to improve this is by exchanging hydrogen atoms with fluorine atoms, which transforms the BH_4^--anion into the BF_4^--anion. But using $Mg(BF_4)_2$ as electrolyte resulted in passivation of the magnesium metal anode.[9] Muldoon *et al.* evaluated different aryl-borate anions with and without fluorine atoms ($[BPh(FPh_3)]^-$, $[B^fAr_4]^-$, $[BPh_4]^-$, $[BPh_3n\text{-}Bu]^-$).[11] Therein, they demonstrated quite easy synthetic approaches (reacting organo magnesium with organo boranes or salt metathesis), but some of their salts still contained chloride integrated within the crystal structure resulting from the precursors. This can again lead to the formation of $MgCl^+$ as redox-active species. The $Mg(BPh_3n\text{-}Bu)_2$ salt showed reversible plating/stripping in a very limited voltage window (up to <2.0 V). With the fluorinated $Mg(B^fAr_4)_2$ salt ($Mg[B(3,5\text{-}bis(trifluoro\text{-}methyl)phenyl)_4]_2$), a high oxidative stability (>4 V vs. SS) was demonstrated. Unfortunately, this salt cannot be used as electrolyte as it is not capable of Mg plating/stripping.

In 2017, Zhao-Karger *et al.* presented the $Mg[B(hfip)_4]_2$ salt as non-corrosive electrolyte, which can be straightforwardly synthesized through the reaction of $Mg(BH_4)_2$ and hexafluoroisopropanol (Hhfip, hfip = $OC(H)(CF_3)_2$).[17] The electrolyte shows remarkable oxidative stability (>4 V vs. SS) and high Coulombic efficiency (>98%). They demonstrated reversible Mg plating/stripping and the compatibility with a sulfur-based cathode. Since its publication, this electrolyte has been utilized for various cathode materials including organic materials (p- and n-type))[61–65] and inorganic materials (sulfur, metal sulfides/oxides).[66–68] In 2020 Mandai showed an optimized synthetic procedure for $Mg[B(hfip)_4]_2$, using a transmetalation reaction between an organo magnesium, borane complex and hexafluoroisopropanol, instead of dehydrogenation of $Mg(BH_4)_2$ with hexafluoroisopropanol.[69]

Dlugatch *et al.* described a conditioning process for this electrolyte. Through electrochemical pretreatment, they could significantly improve the overall performance. Later they could even show that this pretreatment decreases the effect of chloride ions in the electrolyte, especially regarding activation, using Chevrel phase as cathode.[70,71]

In 2019 Luo *et al.* synthesized a perfluorinated pinacolato borate magnesium electrolyte $Mg[B(PFP)_4]_2$ ($Mg\{B[((CF_3)_2CO)_2]_4\}_2$), reacting $Mg(BH_4)_2$ with perfluoro-pinacol.[72] This electrolyte showed also high anodic stability (4.0 V vs. SS) and Coulombic efficiency (95%), but suffers from high price of the precursor and complicated purification procedures. Nevertheless, Pavčnik et al. combined this electrolyte with di-*n*-butyl magnesium and applied this mixture as electrolyte in a

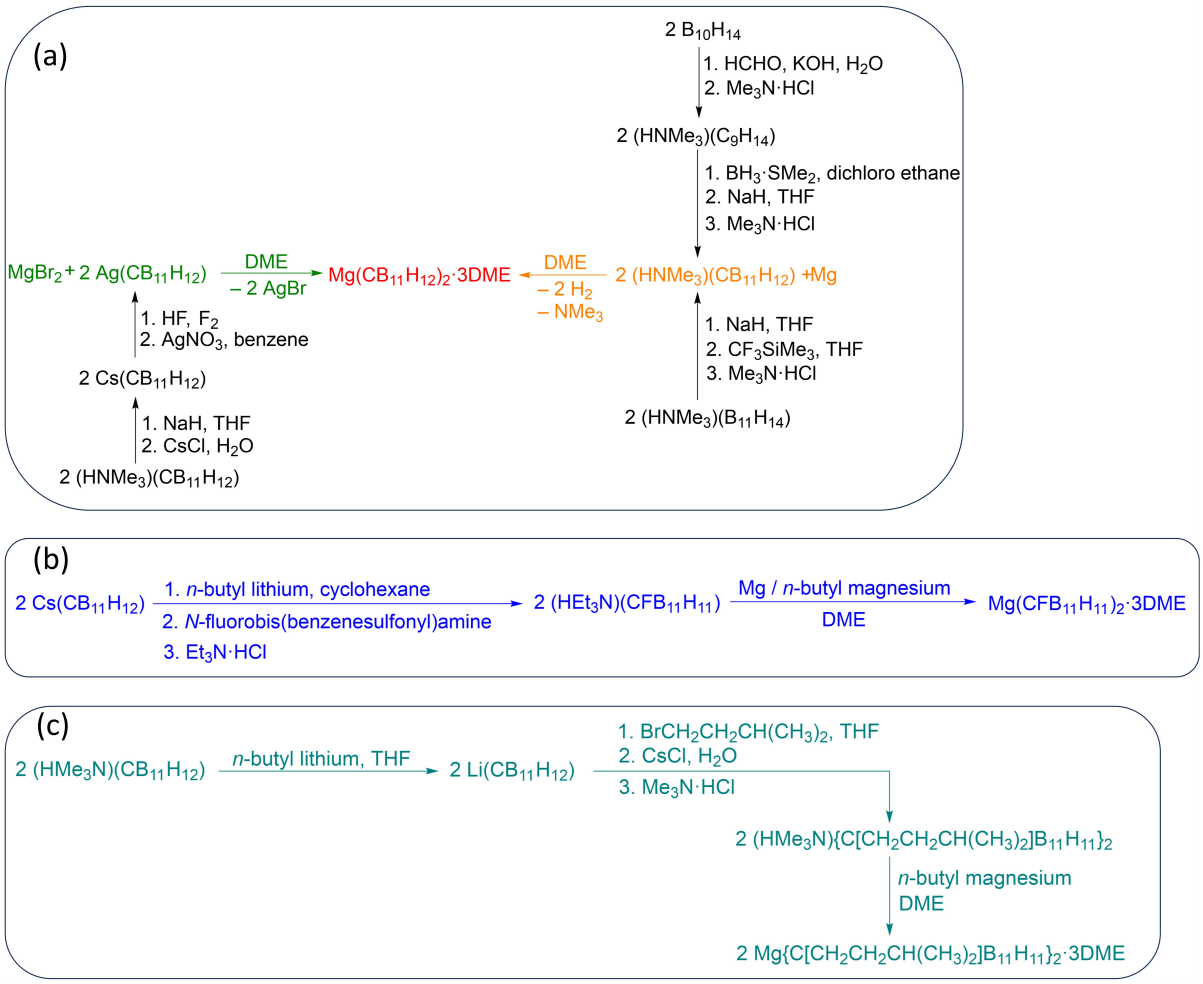

Scheme 2. Various synthetic pathways for the boron clusters described in literature: (a) $Mg(CB_{11}H_{12})_2$: two different paths are listed[18,56–59]; (b) $Mg(CFB_{11}H_{11})_2$ starting from $Cs(CB_{11}H_{12})$[54,60]; (c) $Mg\{C[CH_2CH_2CH(CH_3)_2]B_{11}H_{11}\}_2$ using $(HMe_3N)(CB_{11}H_{12})$ as precursor.[55]

magnesium cell with an organic cathode to show the feasibility of this system.[73]

Another fluorinated anion was presented by Ren *et al.* They synthesized magnesium tetra(trifluoro-ethanoloxy)borate ($Mg[B(OCH_2CF_3)_4]_2$) using a similar procedure as described by Mandai for $Mg[B(hfip)_4]_2$.[74] This electrolyte showed high Coulombic efficiency (~99%), but lower ionic conductivity (0.4 mS cm^{-1} vs. 6.9 mS cm^{-1}) and anodic stability (~3.0 V vs. >4.0 V) compared to $Mg[B(hfip)_4]_2$.

Recently, Li *et al.* presented another synthetic approach towards $Mg[B(hfip)_4]_2$.[75] A cation replacement method was applied, using $Zn(BH_4)_2$ as precursor, which is cheaper than $Mg(BH_4)_2$. However, $Zn(BH_4)_2$ is also synthesized via a chloride precursor.

The different synthetic pathways for $Mg[B(hfip)_4]_2$ are summarized in Scheme 3. Depending on the synthetic approach different trace impurities must be considered, which may affect the electrochemical properties of the prepared electrolytes.

Recently, Huang *et al.* synthesized an asymmetric anion, using $Mg(OTf)_2$ and (tris(2,2,2-trifluoroethyl) borate as starting materials.[76] Dissolving these in DME and adding magnesium powder and catalytic amounts of $CrCl_3$ lead to the desired asymmetric salt $Mg\{B((OCH_2CF_3)_3(OSO_2CF_3)\}_2$. They demonstrated high Coulombic efficiency (98.15%), satisfying anodic stability (3.0 V vs. SS), conductivity (1.38 mS cm^{-1}) and good cyclability (~60 mAh g^{-1}, 600 cycles, 1 C, CE = ~100%) combined with a Chevrel phase cathode. But it is important to consider that traces of chloride may be present, as indicated by their analytical data (*e.g.*: XRD). These traces of chloride have the potential to impact the battery performance.

To obtain a more thorough overview of the different discussed anions and their chemical composition, three-dimensional structures are summarized and displayed in Figure 4.

3.2. Aluminate Mg Salts

Since aluminum is in the same main group as boron, has very similar chemical properties and has already been successfully used in traditional mixed electrolyte salts (as $AlCl_3$ or $AlCl_2R$, Table 1), various anions (Table 2), which are discussed below, have also been developed and tested. In 2016 Herb *et al.* used a

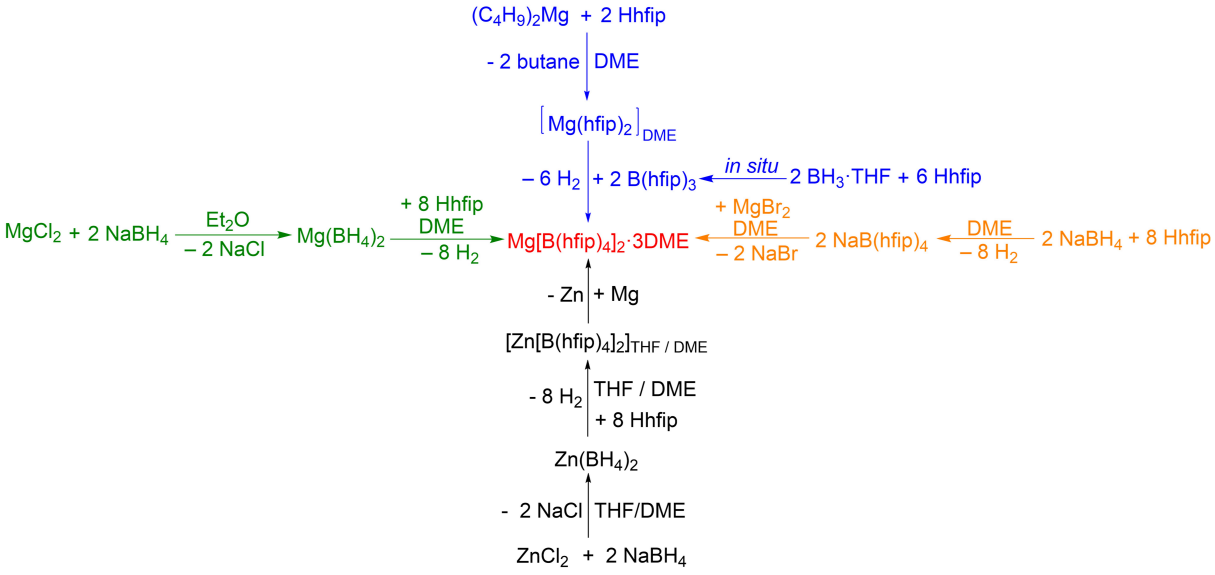

Scheme 3. Different synthetic approaches towards $Mg[B(hfip)_4]_2$.[17,69,75]

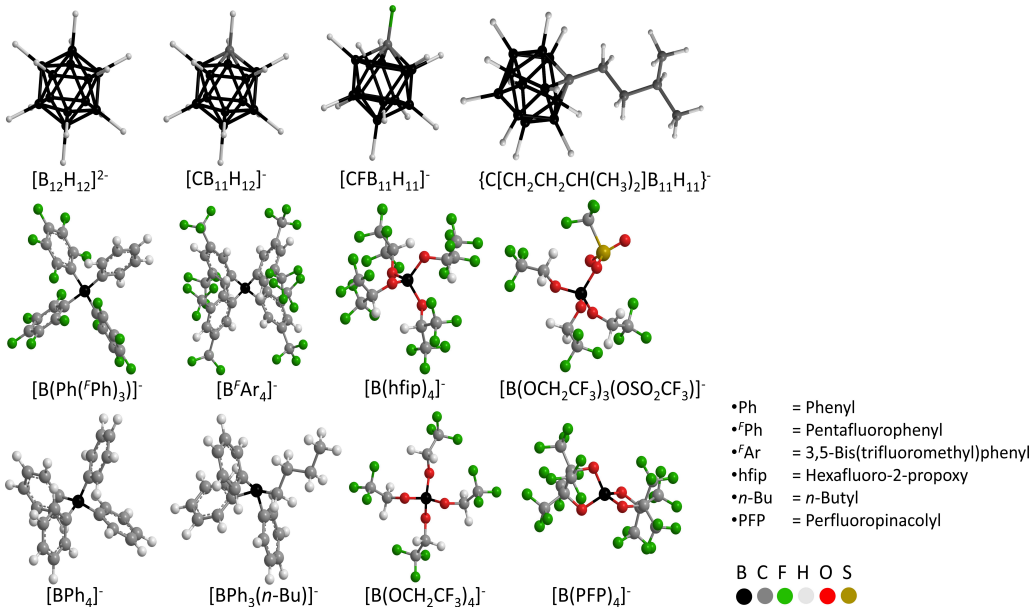

Figure 4. Structures of different borate anions created by Chem3D.

mixture of $[Mg(hfip)_2]$-$[Al(hfip)_3]_2$ in DME as electrolyte, which should form *in situ* $Mg[Al(hfip)_4]_2$. They presented reversible plating/stripping, good conductivities ($>6\ mS\,cm^{-1}$) and a high Coulombic efficiency (99.3 %), thus establishing that magnesium alkoxy aluminates are promising electrolyte candidates for rechargeable magnesium metal batteries.[77]

In 2019 Keyzer *et al.* published a synthesis method to generate different magnesium alkoxy aluminates ($Mg(AlR_4)_2$; R = O*t*-Bu, O*t*-^{F}Bu, hfip, OPh, O^{F}Ph).[78] As shown in Scheme 4 this procedure starts again from a chloride precursor, which leads to contamination in the final products. They took effort in removing any residual chlorides and compared the results. Further investigations were performed on $Mg[Al(Ot\text{-}^FBu)_4]_2$ and $Mg[Al(OPh)_4]_2$, comparing a fluorinated and a non-fluorinated candidate. They were able to demonstrate reversible plating/stripping for both candidates and reached Coulombic efficiencies >90 %. Furthermore, both salts were tested in magnesium cells with Chevrel phase as cathode and showed promising results (~70–95 $mAh\,g^{-1}$, 50 cycles). However, the salts with a higher chloride content performed capacity-wise slightly better (~70 vs. ~95 $mAh\,g^{-1}$), but suffered in anodic stability (~2.1 V vs. ~3.0 V). They attribute the improved capacity to the presence of NaCl, which is why Na^+ can also insert into Chevrel phase and thus increase the overall capacity. In general, this work indicates in particular that the synthetic pathway of alkoxy aluminates

Table 2. List of borate and aluminate Mg electrolytes and summary of their electrochemical properties.

Single salt	Solvent	Ionic conductivity at rt [mS cm^{-1}]	Anodic stability [V]	Efficiency [%]	Ref.
$Mg(BH_4)_2$	DME	–	1.7 vs. Pt	67	[52]
$Mg(CB_{11}H_{12})_2$	tetraglyme	2.9	3.8 vs. Al	94.4	[18]
$Mg(CFB_{11}H_{11})_2$	triglyme	0.14	>4.0 vs Pt	96	[54]
$Mg\{C[CH_2CH_2CH(CH_3)_2]B_{11}H_{11}\}_2$	DME	7.3	4.2 vs.Pt	94.2	[55]
$Mg(BPh_3n\text{-}Bu)_2$	THF	–	<2.0 vs. Pt	96	[11]
$Mg[B(hfip)_4]_2$	DME	6.9	>4.0 vs. SS	>98	[17]
$Mg\{B[((CF_3)_2CO)_2]_4\}_2$	diglyme	3.95	4.0 vs. SS	95	[72]
$Mg[B(OCH_2CF_3)_4]_2$	THF	0.4	>3.0 vs. SS	~99	[74]
$Mg\{B[(OCH_2CF_3)_3(OSO_2CF_3)]\}_2$	DME	1.38	3.0 vs. SS	98.15	[76]
$[Mg(hfip)_2]$-$[Al(hfip)_3]_2$	DME	>6.0	>3.5 vs. Au	99.3	[77]
$Mg[Al(Ot\text{-}Bu)_4]_2$	THF	–	>3.5 vs. Pt	–	[78]
$Mg[Al(Ot\text{-}^tBu)_4]_2$	DME	–	~3.0 vs. Pt	~95–97	[78]
$Mg[Al(hfip)_4]_2$	DME	–	~3.0 vs. Pt	–	[78]
$Mg[Al(OPh)_4]_2$	DME	–	~3.0 vs. Pt	~94–96	[78]
$Mg[Al(O^FPh)_4]_2$	DME	–	<2.0 vs. Pt	–	[78]
$Mg[Al(hfip)_4]_2$	DME	~12.0	~3.5 vs. Pt	99.4%	[79]

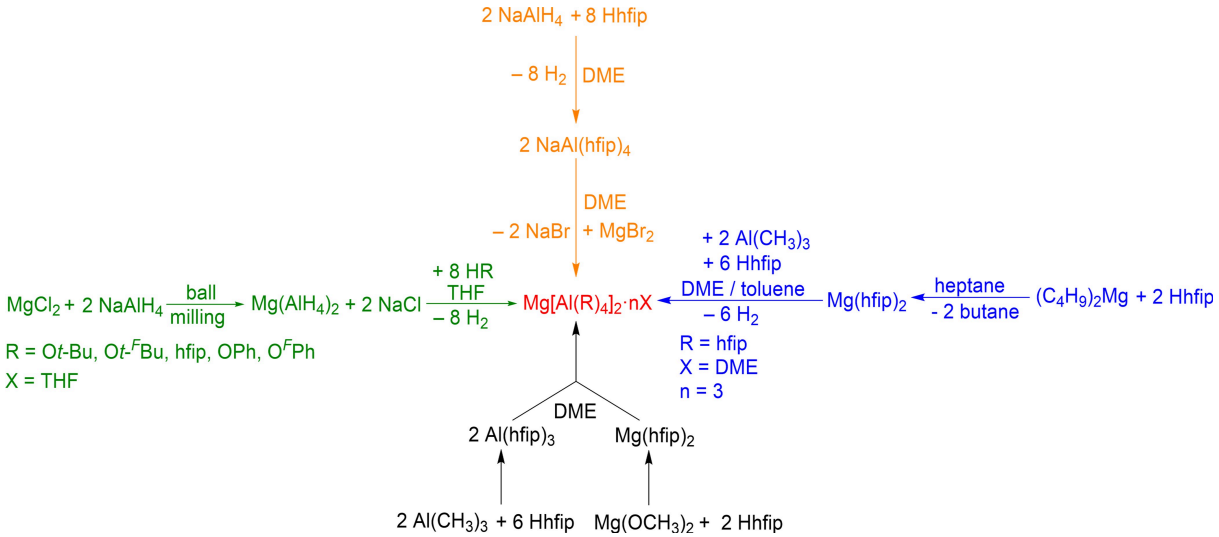

Scheme 4. (green) Synthetic pathway to different magnesium alkoxy aluminates presented by Keyzer *et al.*[78] (blue) Synthetic pathway to $Mg[A(hfip)_4]_2$ by Mandai *et al.*[79] (all) Synthetic pathways compared by Pavčnik *et al.*[80]

must be improved in order to exclude impurities, as these may affect the electrochemical performance.

In 2020 Tang *et al.* presented the synthesis of the perfluorinated pinacolato aluminate magnesium electrolyte $Mg[Al(PFP)_4]_2$ ($Mg\{Al[((CF_3)_2CO)_2]_4\}_2$).[47] Their synthesis started from the reaction between di *n*-butyl magnesium and perfluoro pinacol (H-PFP = $[(CF_3)_2C(OH)]_2$, PFP = $[(CF_3)_2CO]_2$) to obtain $Mg(PFP)_2$ and then they added $AlCl_3$ to get $Mg[Al(PFP)_4]_2$. But because a chloride precursor was used, they yielded $[Mg_2Cl_3][Al(PFP)_2]$ as final product. Therefore, this type of salt is closer related to the complex type of electrolytes as to the single salts (Table 1). Despite that, they could demonstrate reversible Mg plating/stripping, high Coulombic efficiency (~99%) and anodic stability up to ~3.0 V. Furthermore, they described that this salt could form an improved SEI. This was proven by using the cycled Mg anodes (with SEI) in a cell with pure $Mg(TFSI)_2$ as electrolyte. However, as already mentioned, this electrolyte contains large amounts of chlorides, which resembles the drawbacks of the Cl-containing complex electrolytes as discussed above.

Later, Mandai et al. adapted the synthetic approach from Herb *et al.* to produce the pure electrolyte salt $Mg[Al(hfip)_4]_2$,[79] shown in Scheme 4 (blue), without using any chloride precursors. They could show reversible plating/stripping, high Coulombic efficiency (99.4%) and anodic stability (~3.5 V vs. Pt).

Pavčnik *et al.* tested this electrolyte, prepared through the same synthesis as Mandai *et al.* in various magnesium cell

systems with both organic and inorganic cathodes.[81] Later, the same group evaluated the performance of this electrolyte and the costs regarding to the synthetic pathway (Scheme 4).[80] Overall, the approach starting from di *n*-butyl magnesium performed best (Scheme 4, blue), but is the most expensive at the same time.

Hu *et al.* demonstrated again the compatibility of this salt in a magnesium cell with an organic cathode and confirmed the results from Pavčnik *et al.*[81,82]

Furthermore, it has to be considered that the alkyloxyaluminate anion is heavier compared to the alkyloxyborate anion and the extreme water sensitivity of the precursor $Al(CH_3)_3$ require more strict synthesis conditions, which could also affect the cost in a larger scale.[83] To provide a better overview of the various discussed anions and their chemical composition, the three-dimensional structures are summarized and displayed in Figure 5.

3.3. Summary of the Properties of Single Salt Electrolytes

In the past years promising single salts were developed. However, it is crucial to consider the synthesis route, including factors such as contamination and costs. In Figure 6 we compare the different types of single salts, like carboranes, borates and aluminates, regarding their chemical and electrochemical properties. From this overview it is easy to see, why the $Mg[B(hfip)_4]_2$ electrolyte is in our opinion the state-of-the-art electrolyte concerning its chemical and electrochemical properties as well as its synthetic procedure. In Table 2 the electrochemical properties for all discussed single salts are listed.

4. Electrolyte Additives to Optimize Anode/Electrolyte Interfaces

We have already summarized various single magnesium salts developed with high electrochemical and chemical stability, and sufficient ionic conductivity. However, the single salt electrolytes still suffer from the high charge transfer resistance at the Mg surface (due to adsorbed species in the solution, formation of passivation layers, etc.). For this reason, the development is focused on seeking additives that can overcome these problems, in particular the search for additives that can simultaneously activate the magnesium metal surface, but also form a protective interface.

Li *et al.* used the commercial salt $Mg(TFSI)_2$ and added iodine to form a solid MgI_2 layer at the Mg surface.[85] This layer is magnesium ion conductive and led to a decreased polarisation for Mg plating/stripping (+1.87 V/−0.80 V → +50 mV/−170 mV) and in a full cell with a sulfur cathode as well (1.69 V → 0.55 V). However, the Coulombic efficiency is still very low.

Hebié *et al.* also used $Mg(TFSI)_2$ and added anthracene.[86] With this concept they were able to show decreased polarisation (~250 mV) and reversible Mg plating/stripping with satisfying anodic stability (~3.2 V vs. Pt) (Figure 7). But the formed interlayer seems to be not homogenous and stable enough for good long-time stability.

Another approach was done by Horia *et al.* They combined $Mg(HMDS)_2$ with tetrabutylammonium borohydride ($TBABH_4$), which is in this case a moisture and impurity scavenger, and could clean the metal surface.[22] Especially if one considers that otherwise $Mg(HMDS)_2$ only functions with high chloride content, this is a very interesting approach. They reached good Coulombic efficiency (98.3 %) and satisfying ionic conductivity (~0.3 mS cm^{-1}), but suffered a bit in anodic stability (< 3 V vs.

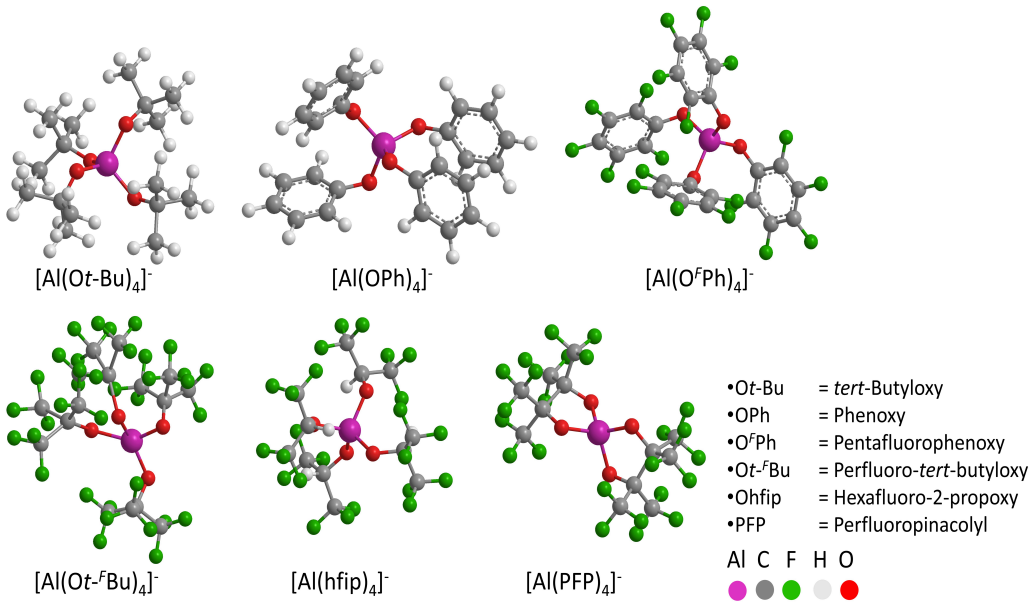

Figure 5. Structures of different aluminate anions created by Chem3D.

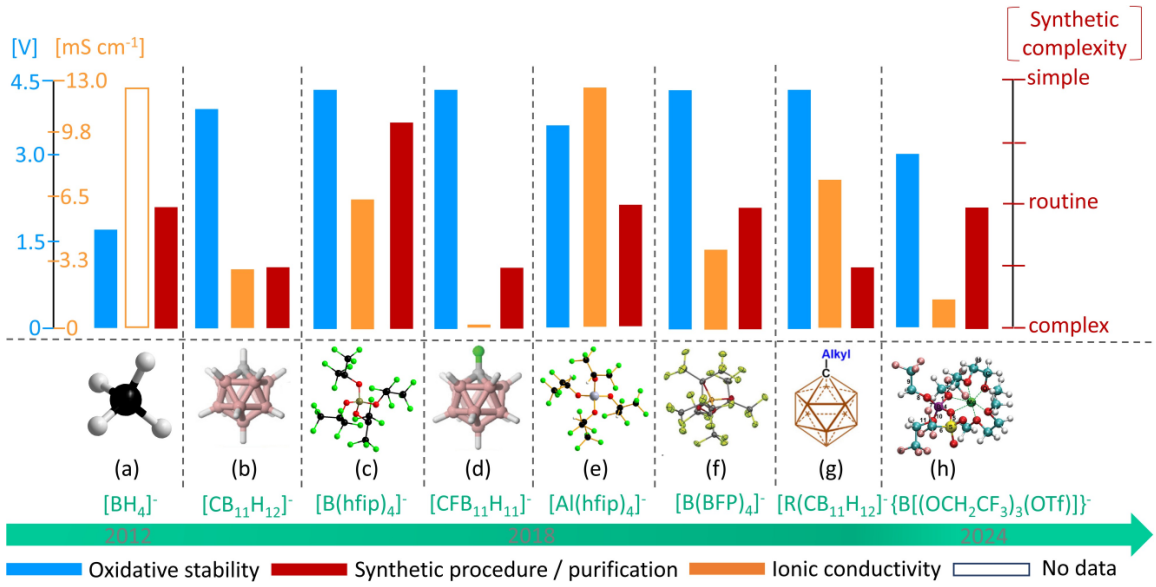

Figure 6. Overview of the development and comparison of boron- and aluminum-based single salts and highlighting their chemical and electrochemical properties: (a) $Mg(BH_4)_2$ (structure created in Diamond 4.0 using published data)[52,84]; (b) $Mg(CB_{11}H_{12})_2$,[18] Reproduced with permission,[54] Copyright © 2018, American Chemical Society; (c) $Mg[B(hfip)_4]_2$ (structure created in Diamond 4.0 using published data)[17]; (d) $Mg(CFB_{11}H_{11})_2$, Reproduced with permission,[54] Copyright © 2018, American Chemical Society; (e) $Mg[Al(hfip)_4]_2$,[78,79,82] Reproduced under terms of the CC-BY license,[81] Copyright © 2018 T. Pavčnik, M. Lozinšek, K. Pirnat, A. Vizintin, T. Mandai, D. Aurbach, R. Dominko, J. Bitenc; Published by American Chemical Society 2022.; (f) $Mg\{B[((CF_3)_2CO)_2]_4\}_2$, Reproduced with permission,[72] © 2019 Wiley-VCH Verlag GmbH & Co. KGaA, Weinheim; (g) $Mg\{C[CH_2CH_2CH(CH_3)_2]B_{11}H_{11}\}_2$, R = $C[CH_2CH_2CH(CH_3)_2$, Reproduced under terms of the CC-BY license,[55] Copyright © 2018 A. W. Tomich, J. Chen, V. Carta, J. Guo, V. Lavallo; Published by American Chemical Society 2024.; (h) $Mg\{B[(OCH_2CF_3)_3(OSO_2CF_3)]\}_2$, Reproduced with permission,[76] Copyright © 2024 Wiley-VCH GmbH.

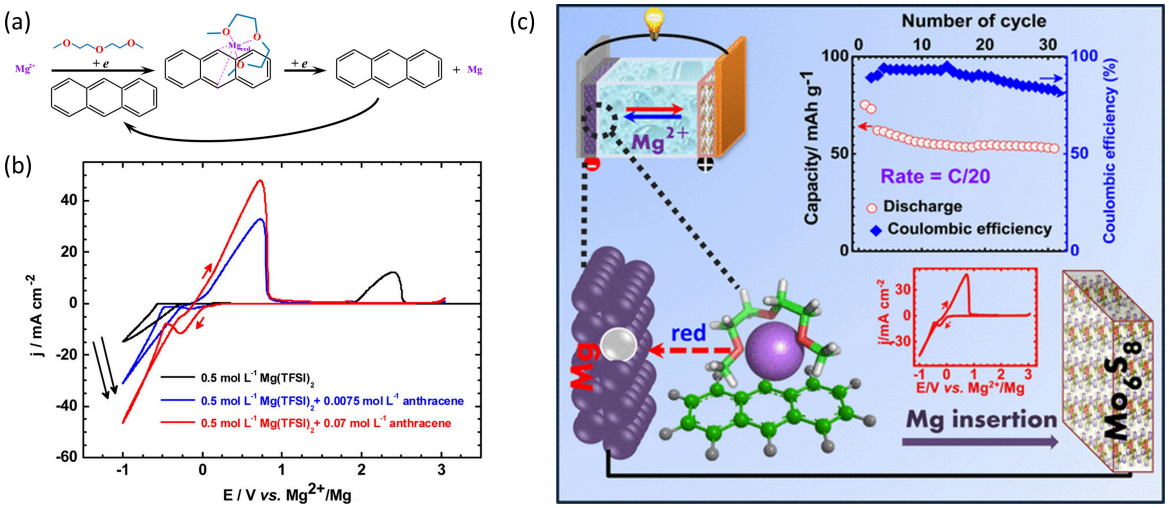

Figure 7. *Electrolyte mixture:* $Mg(TFSI)_2$ + anthracene (a) The proposed Mg(II) reduction mechanism in the presence of anthracene.; (b) Cyclic voltammetry on Pt electrode of diglyme solutions containing different electrolyte compositions (V = 50 mV s^{-1} at 25 °C).; (c) Schematic illustration of the $Mg(TFSI)_2$ + anthracene concept (red: reduction). Reproduced with permission,[86] Copyright © 2018, American Chemical Society.

Al). Furthermore, the polarisation in symmetrical cell is still quite high (~500 mV, Figure 8d).

Li *et al.* used $Mg(BH_4)_2$ as additive for the state-of-the-art $Mg[B(hfip)_4]_2$ electrolyte.[21] Similar as $TBABH_4$, $Mg(BH_4)_2$ serves as a moisture scavenger. Furthermore, it can remove the native oxide layer from the Mg metal anode and boosts the formation of a stable anode/electrolyte-interface. They demonstrated reversible cycling for 600 cycles using this mixture and a Chevrel phase cathode. The electrolyte mixture showed high Coulombic efficiency (>99%) and low polarisation (~100 mV), but suffer again in anodic stability (~2.8 V vs. Pt) (Figure 9). The decreased anodic stability can be traced back to the BH_4^- anion, which is known for its low anodic stability.[52]

Meng *et al.* chose another additive $Bi(OTf)_3$, still using the benchmark magnesium electrolyte $Mg[B(hfip)_4]_2$.[20] As described, this compound can react with the magnesium metal anode, forming *in situ* a mixture of an alloy (Mg_3Bi_2) and bismuth as a thin layer on the magnesium surface. This layer

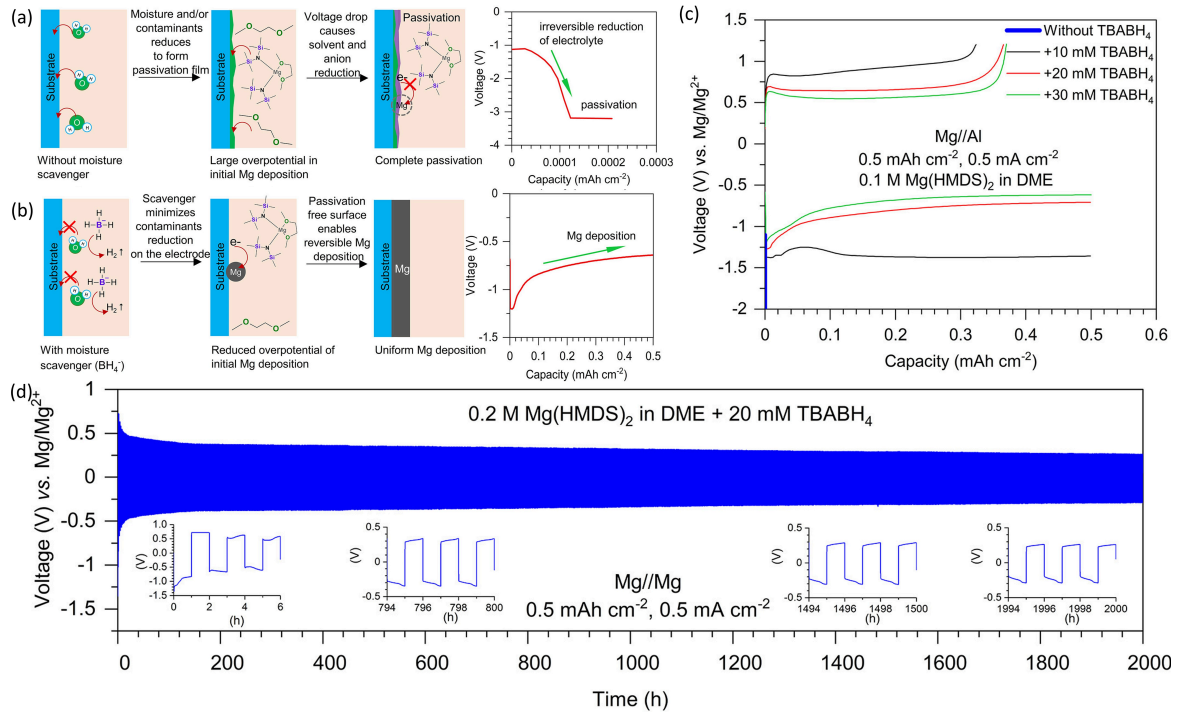

Figure 8. *Electrolyte mixture:* $Mg(HMDS)_2 + TBABH_4$ (a and b) Schematic illustration of magnesium deposition process without (a) and with (b) moisture scavenger in the electrolyte. The voltage limit for the plating process is set at −3.25 V. Upon reaching this limit, the constant voltage was held at −3.25 V until the end of plating.; (c) Effect of $TBABH_4$ on the reversibility of Mg plating/stripping: Voltage profile of the first Mg deposition/dissolution cycle in 0.1 m $Mg(HMDS)_2$ in DME with addition of $TBABH_4$.; (d) Stable cycling of a symmetrical cell. Reproduced with permission,[22] Copyright © 2021, American Chemical Society.

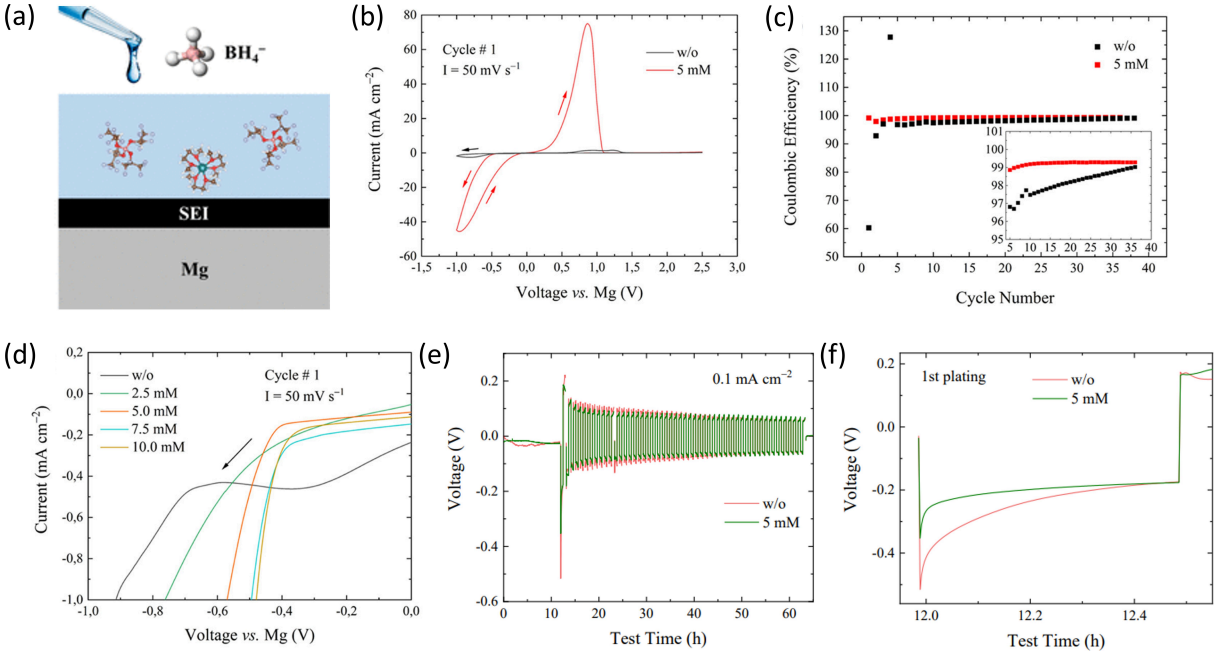

Figure 9. *Electrolyte mixture:* $Mg[B(hfip)_4]_2 + Mg(BH_4)_2$ (a) Schematic illustration of the applied mixture.; (b) Comparison of the first CV cycle with and without additive.; (c) Coulombic efficiency of Mg stripping/plating with and without additive.; (d) Initial Mg plating in the first cycle CV scan with various amount of additive.; WE was Pt in all measurements.; (e and f) Chronopotentiometry of Mg//Mg symmetric cells with (green) and without (red) additive: (e) from rest to cycle 50; (f) first plating.; Reproduced under terms of the CC-BY license,[21] Copyright © 2018 Z. Li, T. Diemant, Z. Meng, Y. Xiu, A. Reupert, L. Wang, M. Fichtner, Z. Zhao-Karger. Published by American Chemical Society 2021.

protects the magnesium metal surface by reducing the adsorption of inactive species on the Mg surface, thus preventing passivation. At the meantime, the charge transfer is promoted during the on-off transition, as Mg_3Bi_2 shows high

Mg^{2+} conductivity.[87] This effect is evident in high current response (~80 mA cm^{-2}) and high Coulombic efficiencies (~99%) can be observed during plating/stripping from the beginning (Figure 10). Furthermore, testing symmetrical cells demonstrated that the polarisation is already reduced in the first cycles and reaches a stable value fastly (~140 mV). Coupling the system with a Chevrel phase cathode showed again the beneficial effect in decreasing the polarisation (320 mV → 140 mV).

A similar attempt was done by Yang *et al.*[88] They mixed $Mg(OTf)_2$ with $InCl_3$ and observed the formation of a mixture of indium and magnesium-indium-alloys at the magnesium metal surface. They defined these alloys as magnesiophilic sites, which led to a more uniform Mg deposition. Reversible Mg plating/stripping was demonstrated with high Coulombic efficiency (98.7%) and the symmetrical cells showed low polarisation (~150 mV). Full cells with Chevrel Phase as cathode were cycled with high capacity retention for 800 cycles. Comparisons with $MgCl_2$ instead of $InCl_3$ demonstrated the improved overall performance (*e.g.*: initial polarisation in Mg//Mg cells: 230 mV vs. 980 mV) of the magnesium-indium-mixture, but the anodic stability, which was not mentioned, would be important for further application. Furthermore, as already discussed in the previous chapters, even small amounts of chloride ions can lead to the formation of $MgCl^+$ species and therefore to a different system.

Xie *et al.* combined phenyl disulfide ($C_6H_5S_2C_6H_5$) with the standard $Mg(HMDS)_2/MgCl_2$-mixture, achieving a satisfying ionic conductivity (~1.25 mS cm^{-1}).[89] With that combination they were able to improve the polarisation (~41 mV) and stability in symmetrical cells. Furthermore, for asymmetric cells the Coulombic efficiency increased from 96.9% to 99.5%. *Post mortem* analysis of the anode showed a more uniform surface with an organic-rich layer, which is ion conductive and can prevent the Mg anode from further passivation.

A chloride-free approach was presented by Chinnadurai *et al.*[19] Combining $Mg(OTf)_2$ and $Mg(HMDS)_2$ with tetrabutylammonium triflate (TBAOTf) as additive, the electrolyte showed a high anodic stability (4.43 V vs. Pt), satisfying polarisation (< 500 mV) and improved Coulombic efficiency (> 90%) (Figure 11). From their analytical results, two layers are formed at the Mg metal surface, a MgF_2-rich layer and at the top an organic-rich layer, which are robust and conductive and lead to uniform Mg deposition.

A comparable, but Cl-containing concept, was applied by Nguyen *et al.* Using a mixture of $Mg(OTf)_2$ and tetrabutylammonium chloride (TBACl) they achieved a ionic conductivity of ~2.5 mS cm^{-1}.[90] They also described the formation of two layers, one inorganic ($MgCl_2/MgF_2$/Mg oxides) and one organic layer. The cells presented low polarisation over a long time period in symmetrical cells (290 mV, 600 h) and demonstrated

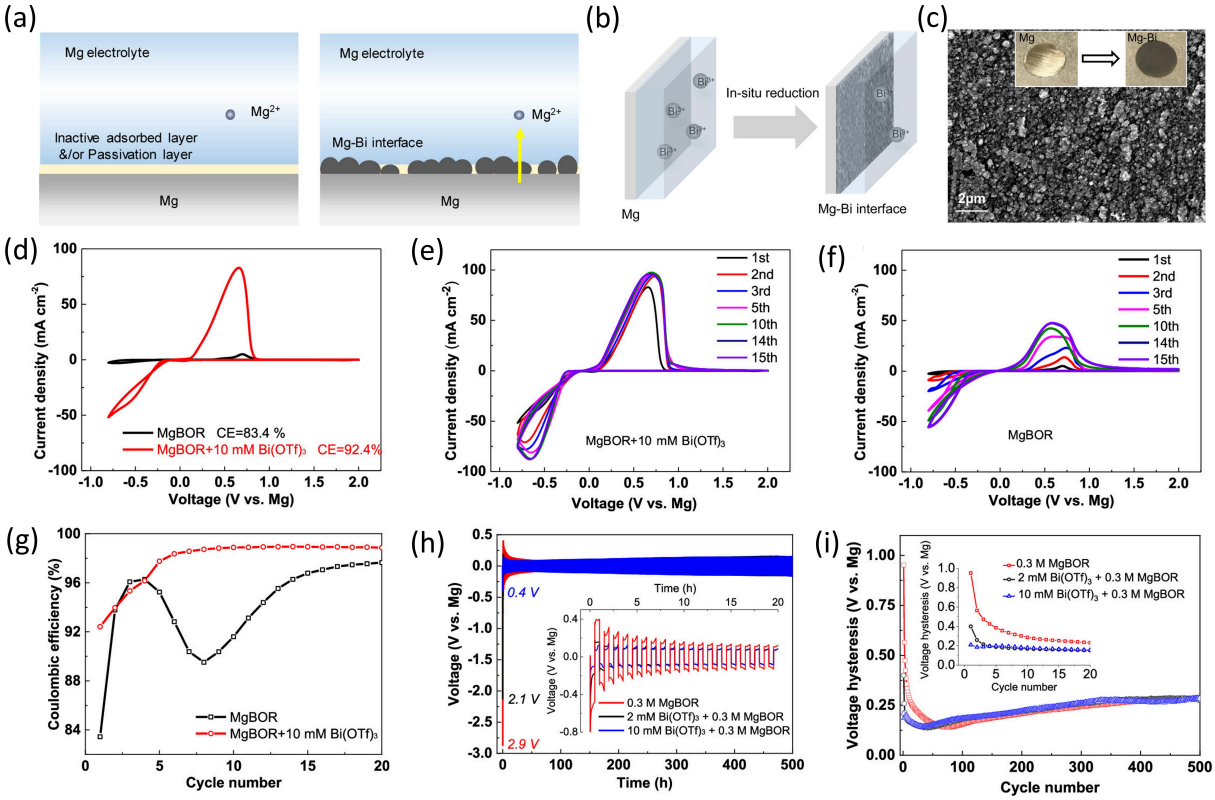

Figure 10. *Electrolyte mixture:* $Mg[B(hfip)_4]_2$ + $Bi(OTf)_3$ (a) Schematic illustration of the layer at the Mg surface without and with additive.; (b) Scheme of the *in situ* reaction taking place at the Mg surface.; (c) SEM image of the Mg–Bi interface and pictures of Mg anode before and after treatment with the additive.; (d) Comparison of the first cycles of stripping/plating with and without additive.; (e and f) The first 15 cycles of CV with (e) and without (f) additive.; (g) Corresponding Coulombic efficiency with and without additive.; (h und i) Symmetrical cells with and without additive and corresponding voltage hysteresis.; Reproduced with permission,[20] Copyright © 2021, American Chemical Society.

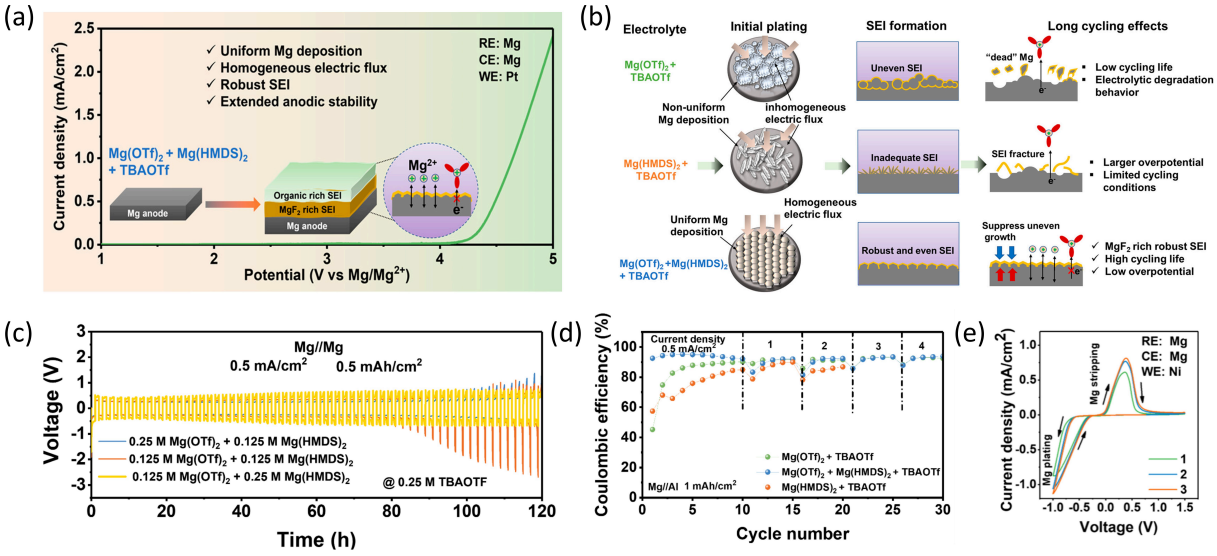

Figure 11. *Electrolyte mixture:* $Mg(OTf)_2 + Mg(HMDS)_2 + TBAOTf$ (a) Overview about the beneficial effects of this electrolyte mixture; (b) Schematic illustrations of Mg deposition in different electrolyte mixtures; (c) Comparison of the polarisation of Mg//Mg symmetrical cells using different electrolyte mixtures.; (d) Coulombic efficiencies at different current densities and electrolyte compositions; (e) Cyclic voltammetry: Mg//Ni at a scan rate of 10 mV s^{-1}.; Reproduced with permission[19] Copyright © 2023, American Chemical Society.

Table 3. List of enhanced salt-additive mixtures and a summary of their reported electrochemical properties.

Conductive salt(s)	Additive	Solvent	Polarisation [mV]	Anodic stability [V]	Efficiency [%]	Ref.
$Mg(TFSI)_2$	I_2	DME	+50/−170	–	–	[85]
$Mg(TFSI)_2$	anthracene	diglyme	~250	~3.2 vs. Pt	–	[86]
$Mg(HMDS)_2$	$TBABH_4$	DME	~500	< 3.0 vs. Al	98.3	[22]
$Mg[B(hfip)_4]_2$	$Mg(BH_4)_2$	DME	~100	~2.8 vs. Pt	99.3	[21]
$Mg[B(hfip)_4]_2$	$Bi(OTf)_3$	DME	~140	–	~99.0	[20]
$Mg(OTf)_2$	$InCl_3$	DME	~150	–	98.7	[88]
$Mg(HMDS)_2$-$MgCl_2$	$C_6H_5S_2C_6H_5$	THF	~41	–	99.5	[89]
$Mg(HMDS)_2$-$Mg(OTf)_2$	TBAOTf	DME/triglyme	< 500	4.43 vs. Pt	–	[19]
$Mg(OTf)_2$	TBACl	DME	290	~2.7 vs. Pt	97.7	[90]
$Mg(HMDS)_2$	$TBABH_4 + MgBr_2$	DME	390	3.1 vs. Pt	99.0	[91]

good Coulombic efficiency (97.7%). However, this combination has a low anodic stability (< 3.0 V) due to the chloride content.

Another chloride-free concept was demonstrated by Chinnadurai *et al.*[91] The commercial salt $Mg(HMDS)_2$ was mixed with two additives, $TBABH_4$ and $MgBr_2$. This mixture resulted in the formation of an inorganic layer and above an organic layer on top at the Mg surface, which lead to uniformly deposited magnesium. However, it should be noted that bromide ions could have similar positive and negative effects as chloride ions. Nevertheless, they presented satisfying polarisation (390 mV) and anodic stability (3.1 V vs. Pt), good Coulombic efficiencies (99%), and long-time stabilities (stable cycling Mg//Mg ~400 cycles).

The properties of the discussed electrolyte mixtures are summarized in Table 3. It is shown that additives can boost the performance of single salts. The electrolytes based on commercial salts such as $Mg(HMDS)_2$, $Mg(TFSI)_2$ and $Mg(OTf)_2$ could be improved by adding additives other than $MgCl_2$. In addition, the system with the benchmark electrolyte $Mg[B(hfip)_4]_2$ could be further enhanced by different additives. Despite the consideration of numerous parameters, there is still potential for ongoing enhancements in the pursuit of an optimal system for broad application.

5. Development of Polymer Electrolytes

Another focus of electrolyte development is the search for solid or quasi-solid electrolytes to improve the stability and safety of the battery systems. Already in 1998, Liebenow presented a magnesium ion conducting polymer electrolyte.[92] They mixed ethyl magnesium bromide and poly(ethylene oxide) (PEO) in THF or di-*n*-butylether (DBE) and after the solvent was evaporated, gel-like systems were obtained. They demonstrated reversible plating/stripping for the THF version at 25 °C (Figure 12a). However, the current response was very low, at

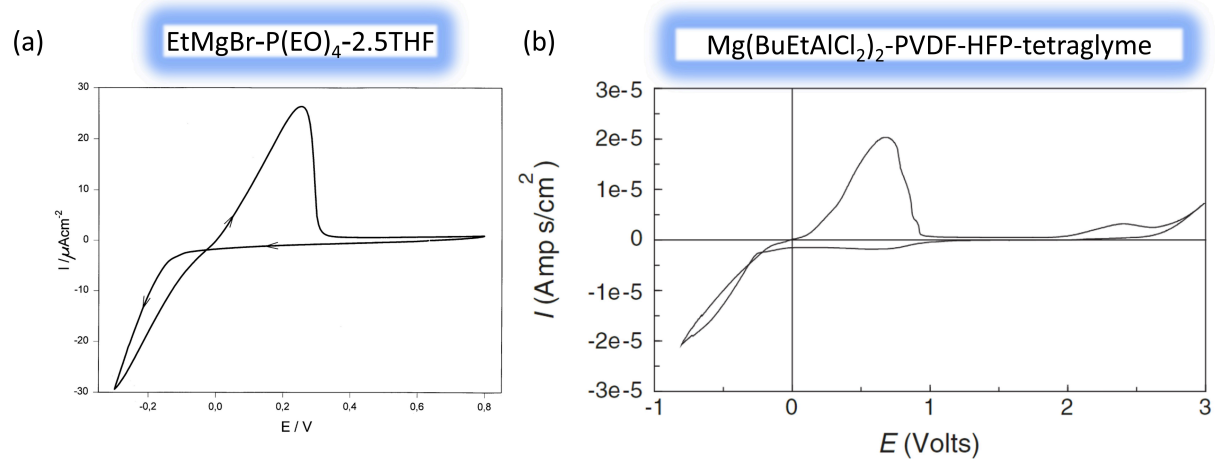

Figure 12. (a) Successful stripping/plating (Mg//Ni) using EtMgBr–P(EO)4-2.5THF as polymer electrolyte by Liebenow. Reproduced with permission,[92] Copyright © 1997 Elsevier Science Ltd. All right reserved.; (b) Cyclic voltammogram (Mg//Au) for $Mg(BuEtAlCl_2)_2$-PVDF-HFP-tetraglyme polymer electrolyte by Chusid *et al.* Reproduced with permission,[94] Copyright © 2003 WILEY-VCH Verlag GmbH & Co. KGaA, Weinheim.[92,94]

around 28 $\mu A\,cm^{-2}$. The presented ionic conductivities are also at low values, even at higher temperatures. ($<0.1\ mS\,cm^{-1}$, 90 °C).

Yoshimoto *et al.* synthesized a gel polymer electrolyte using a poly(ethylene oxide)-modified poly(methacrylate) (PEO-PMA) polymer backbone, with $Mg(TFSI)_2$ and alkyl carbonates as plasticizers, resulting in a mechanically stable self-standing film.[93] They reached a promising conductivity of $2.8\ mS\,cm^{-1}$ at 20 °C and demonstrated the applicability of this gel polymer electrolyte in MgV_2O_5/V_2O_5 (~70 $mAh\,g^{-1}$, 5 cycles) and MgV_2O_5/MnO_2 (~45 $mAh\,g^{-1}$, 5 cycles) cells.

Chusid *et al.* combined $Mg(BuEtAlCl_2)_2$ with different polymers (PVDF-HFP, PEO) and different solvents as plasticizers (tetraglyme, THF).[94] The conductivity of $Mg(BuEtAlCl_2)_2$-PVDF-HFP-tetraglyme was $3.7\ mS\,cm^{-1}$ at 25 °C, which is comparable to that of lithium salt solutions.[95,96] They presented reversible plating/stripping (Figure 12b) and good cyclability in a Mg//Mo_6S_8 cell (80 $mAh\,g^{-1}$; 5 cycles). However, the application is limited to non-electrophilic cathode materials.

Pandey *et al.* used the $Mg(ClO_4)_2$ salt, PVDF-HFP as polymer, MgO-nano particle as filler and alkyl carbonates as plasticizers.[97] They described a high ionic conductivity of $8.0\ mS\,cm^{-1}$ at 25 °C and good anodic stability (~3.5 V vs. SS). Later the same group replaced the MgO to SiO_2 particles to reach a system, which was able to show even higher ionic conductivity of $11.0\ mS\,cm^{-1}$ at 25 °C with still the same anodic stability.[98]

Ford *et al.* have developed a cross-linked ionomer gel separator to mitigate the polysulfide shuttle in magnesium-sulfur batteries.[28] As polymers poly(ethylene glycol) diacrylate (PEGDA) and poly(ethylene glycol) dimethacrylate (PEGDMA) were used, as ionic monomers sodium 4-vinylbenzenesulfonate (NaSS) and potassium 4-styrenesulfonyl(trifluoromethanesulfonyl) imide (KSTFSI) were chosen. One polymer and one ionic monomer were mixed in DMSO and copolymerized using a photo initiator. After that the sodium- or potassium ions were exchanged to magnesium ions, reaching the following compositions: [PEGDA-STFSIMg], [PEGDA-SSMg], [PEGDMA-STFSIMg] and [PEGDMA-SSMg]. The prepared self-standing films were swollen in different magnesium electrolyte solutions or pure THF, and then used as gel polymer electrolytes. The ionic conductivities of the films swollen in pure THF are quite low (10^{-6}–$10^{-4}\ mS\,cm^{-1}$). However, the films swollen in Mg electrolytes exhibited significantly higher conductivities up to $15\ mS\,cm^{-1}$. Using the composition [PEGDA-STFSI–Mg]-Mg-$(TFSI)_2$-$MgCl_2$-DME in a magnesium-sulfur cell demonstrated the applicability of the approach (Figure 13a–c). However, the use of electrolytes containing chloride leads to the problems already discussed above.

Sharma *et al.* presented a chloride-free approach, using a combination of $Mg(OTf)_2$ salt, PVDF-HFP as polymeric backbone, succinonitrile as plasticizer and the ionic liquid 1-ethyl-3-methylimidazolium trifluoromethanesulfonate (EMIOTf) as additive to stabilize the gel polymer.[99] They achieved free-standing films with good conductivity at rt ($4.0\ mS\,cm^{-1}$) and high anodic stability (~4.1 V vs. SS). Furthermore, they presented the cyclability in a Mg//MnO_2 cell (initial capacity: 40 $mAh\,g^{-1}$, 8 cycles).

Another promising approach involves using a single-ion conductor in the polymer electrolyte. By incorporating the anion into the polymer structure, the single ion conducting polymer electrolyte is expected to achieve a high Mg^{2+} transference number.

Merril *et al.* reported a single ion conducting polymer electrolyte, where the anion is covalently bonded to the polymer backbone.[100] For the synthesis, a similar concept as Ford *et al.* have used, was applied.[28] They copolymerized PEGDMA and KSTFSI and exchanged the potassium ion to magnesium, forming a self-standing film. As Ford *et al.* have shown poor conductivities for films only swollen in pure THF, they investigated different solvents (Figure 13d–f) and achieved a good ionic conductivity for DMSO (~$1.0\ mS\,cm^{-1}$ at rt). Unfortunately, they did not demonstrate the Mg stripping/plating behaviour with this single ion conducting electrolyte.

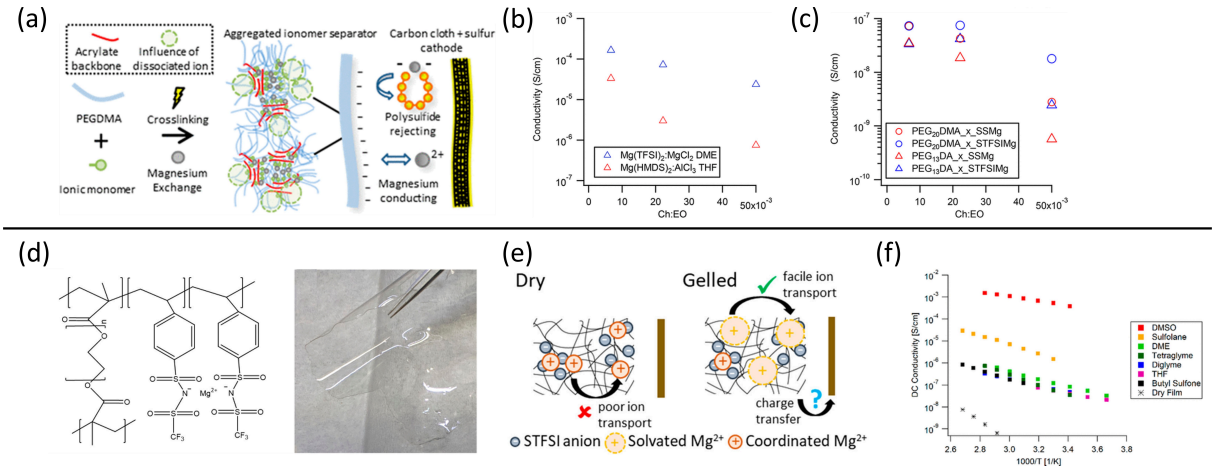

Figure 13. (a–c) Ford *et al.*: (a) Schematic formation of the cross-linked ionomer gel separator and the working principle in a Mg//S cell; (b) Ionic conductivity of PEGDA-STFSI–Mg films swollen in different chloride containing electrolytes; (c) Ionic conductivity of different films swollen in THF.; Reproduced with permission,[28] Copyright © 2018, American Chemical Society; (d–f) Merril *et al.*: (d) Structural schematic of the statistically copolymerized and magnesiated PEGDMA-STFSI network and optical image of the freestanding polymer film; (e) Schematic illustration of the single-ion conducting gel polymer electrolyte; (f) Ionic conductivities of films swollen in different solvents at different temperatures.; Reproduced with permission,[100] Copyright © 2019, American Chemical Society.

Sharma *et al.* also used PVDF-HFP as polymeric backbone and evaluated the effect of different fillers.[25] The standard film consists of $Mg(OTf)_2$, PVDF-HFP und a mixture of ethylene carbonate and propylene carbonate. Al_2O_3 and $MgAl_2O_4$ were investigated as fillers. They reached good ionic conductivities at rt with both fillers (Al_2O_3: 3.3 mS cm^{-1}; $MgAl_2O_4$: 4.0 mS cm^{-1}) and good anodic stability (~3.3 V vs. SS).

An *in situ* crosslinking reaction was applied by Du *et al.* during cell assembly, which enhances the contact between the electrode and the electrolyte.[101] Two solutions were prepared: $Mg(BH_4)_2$ and $MgCl_2$ were dissolved in THF and polytetrahydrofuran (PTHF) was dissolved in THF as well. Both solutions were dropped in sequence onto the glass fiber (GF/A) separator, which works as a skeleton, forming a polymeric network *in situ* (Figure 14). With this gel polymer electrolyte (GPE), the cells demonstrated reversible plating/stripping, low polarisation in symmetrical cells (~100 mV), reasonable ionic conductivity at rt (0.476 mS cm^{-1}) and successful cyclability of a Mg//Mo_6S_8 cell (~75 mAh g^{-1}, 250 cycles).

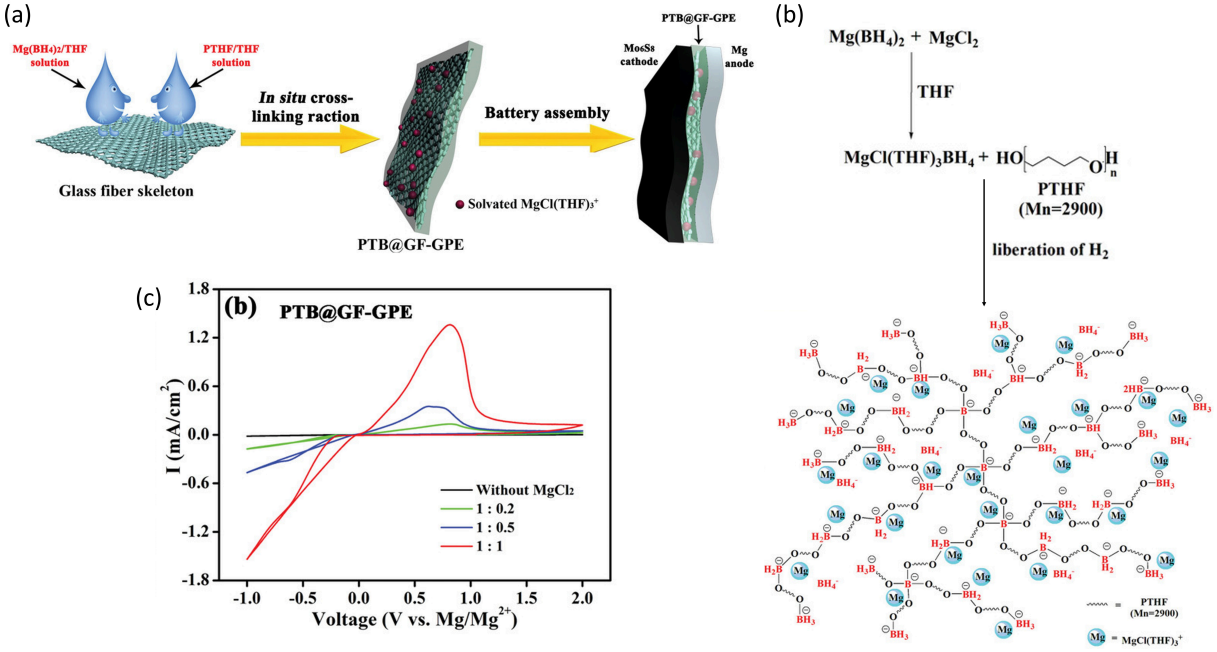

Figure 14. (a) Schematic illustration of the *in situ* preparation of PTB@GF-GPE and the cell assembly procedure; (b) The synthetic route of PTB-GPE based on the reaction of $Mg(BH_4)_2$, $MgCl_2$, and PTHF; (c) Cyclic voltammograms (Mg//SS) using PTB@GF-GPEs with different compositions of $Mg(BH_4)_2$:$MgCl_2$.; Reproduced with permission,[101] Copyright © 2019 WILEY-VCH Verlag GmbH & Co. KGaA, Weinheim.

Fan *et al.* investigated a similar approach as Du *et al.*[24] Instead of crosslinking PTHF, they used fluorinated tetraethylene glycol (FTG). Again, two separate solutions were prepared, then the FTG-THF-solution was added onto the glass fiber separator first, followed by $MgClBH_4$-THF-solution. The separator was stored in a sealed container for 24 hours and then extra THF was added to complete the reaction (Figure 15). Afterwards the separator was allowed to dry at rt. It also showed reversible Mg plating/stripping, low polarization (~180 mV), high Coulombic efficiency (~100 %), and high anodic stability (4.8 V vs. Pt). Furthermore, they synthesized a lithium ion containing version of their GPE adding LiTFSI into the $MgClBH_4$-THF-solution. This hybrid electrolyte demonstrated a good compatibility with a sulfur cathode (~1000 mAh g^{-1}, 50 cycles).

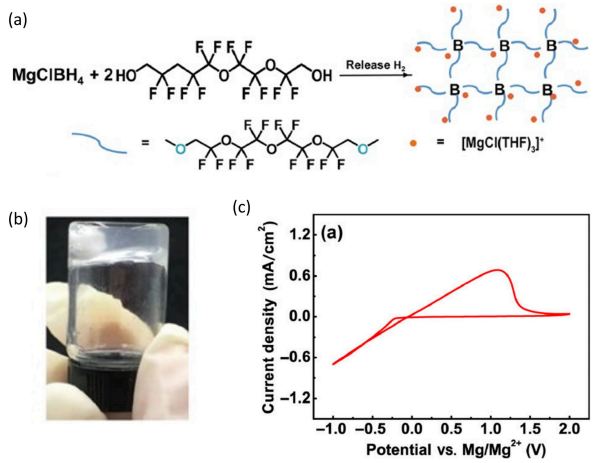

Figure 15. (a) Schematic illustration of the crosslinking reaction; (b) optical image of the formed gel; (c) Cyclic voltammetry of a Mg//Pt cell using the polymer electrolyte.; Reproduced with permission,[24] Copyright © 2020 Tsinghua University Press and Springer-Verlag GmbH Germany, part of Springer Nature.

Mahalakshmi *et al.* studied a combination of cellulose acetate (CA) and magnesium nitrate hexahydrate as polymer electrolyte.[102] The salt and the polymer were dissolved individually in DMF, then the two solutions were mixed and finally the solvent was removed. A mechanically stable transparent film was obtained. A room-temperature conductivity of 0.919 mS cm^{-1} was demonstrated with a quite high anodic stability (3.65 V vs. SS). Park *et al.* did investigations in Mg-$(TFSI)_2$-based polymer electrolytes.[103] As polymers poly(ε-caprolactone-co-trimethylene carbonate) (PCL-PTMC) and poly(ethylene oxide) (PEO) were evaluated, but for both systems the ionic conductivities even at 60 °C were still quite low (~0.1 mS cm^{-1}).

Wang *et al.* used again an *in situ* polymerisation approach, but compared to the attempts before, this approach is chloride-free.[26] They applied the benchmark single salt $Mg[B(hfip)_4]_2$ in their system. Two solutions were prepared: one containing $Mg(BH_4)_2$ and $Mg[B(hfip)_4]_2$ dissolved in DME, and the other containing polytetrahydrofuran (PTHF) dissolved in DME as well. Both solutions were mixed and dropped onto the glass fiber (GF/C) separator, acting as a skeleton. A polymeric network will be formed *in situ* (Figure 16). This $Mg[B(hfip)_4]_2$-based gel polymer electrolyte presented a good ionic conductivity (~2.0 mS cm^{-1}), a high Coulombic efficiency (~99 %, 1000 cycles) and reversible Mg plating/stripping with a low polarisation (~60 mV). Simultaneously, it was demonstrated that the poly-

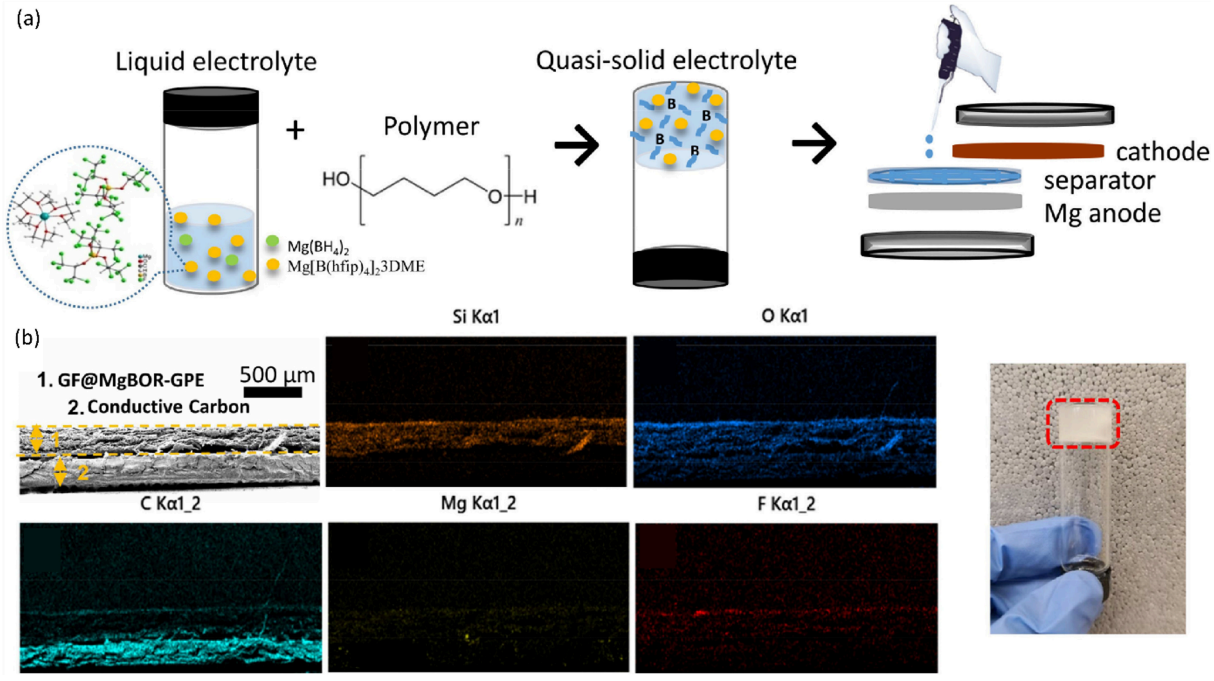

Figure 16. (a) Schematic illustration of the preparation for the gel polymer electrolyte; (b). The cross-section SEM image and EDS maps of glass fiber membrane coated with the gel polymer electrolyte. And an optical photograph of the synthesized electrolyte.; Reproduced with permission[26]; Copyright © 2022 Elsevier B.V. All rights reserved.

meric matrix can effectively prevent dissolution and diffusion of soluble electrode materials. Full cell tests with both sulfur (500 mAh g^{-1} after 20 cycles vs. ~190 mAh g^{-1}) and Chevrel phase as cathode showed improved stability. Finally, the feasibility of the system was further validated in a Mg–S pouch cell (Figure 17).

Wang *et al.* extended their work to another polymeric backbone, still using the single salt $Mg[B(hfip)_4]_2$. The monomer pentaerythritol tetraacrylate (PETEA) was polymerised utilizing AIBN (azobisisobutyronitrile) as initiator inside the electrolyte solution in DME. The resulting solution was dropped onto the glass fiber (GF/C) separator, acting again as a skeleton. The assembled coin cell was heated at 65 °C for 30 min and the polymeric network was formed *in situ* inside the cell. The polypentaerythritol tetraacrylate (PPETEA) based GPE demonstrated reversible Mg plating/striping and a slightly higher ionic conductivity (3.42 mS cm^{-1}) compared to the PTHF based GPE. Furthermore, the anodic stability improved (~3.0 V to ~4.0 V vs. SS) while maintaining the high Coulombic efficiency (~99%). The enhanced anodic stability is attributed to the absence of $Mg(BH_4)_2$ in the system, which, as mentioned above, has a lower anodic stability.

However, the polarisation in symmetrical cells was roughly doubled (~120 mV). Nevertheless, full cell tests with a sulfur cathode (~210 mAh g^{-1} after 50 cycles) demonstrated the feasibility of this GPE (Figure 18). All results confirm that Cl-free Mg GPE's provide promising properties in terms of conductivity and cycling stability, especially in the field of Mg–S batteries.

Another *in situ* approach was presented by Wang *et al.* in a Li–Mg hybrid system.[104] They used a mixture of $Mg(BH_4)_2$, $LiBH_4$, TiO_2 and PTHF in diglyme solvent, which underwent *in situ* crosslinking inside the glass fiber separator. This electrolyte demonstrated reversible Mg plating/stripping, low polarisation (~50 mV), high Coulombic efficiency (99.8%), and anodic stability (~3.5 V). However, it needs to be mentioned that this electrolyte composition consists of fifteen times more lithium ions as magnesium ions. For further application a deeper investigation of the effect/role of lithium ions would be beneficial. Combining this electrolyte with a sulfurized polyacrylonitrile (SPAN) cathode yielded promising results (~750 mAh g^{-1}, 140 cycles), even in a small pouch cell. Later, Sundermann *et al.* developed a polymer electrolyte based on poly(2-butyl-2-ethyltrimethylene-carbonate) (P(BEC)) with either $Mg[B(hfip)_4]_2$ or $Mg(TFSI)_2$ as magnesium salt.[27] At higher temperatures they observed reasonable ionic conductivities

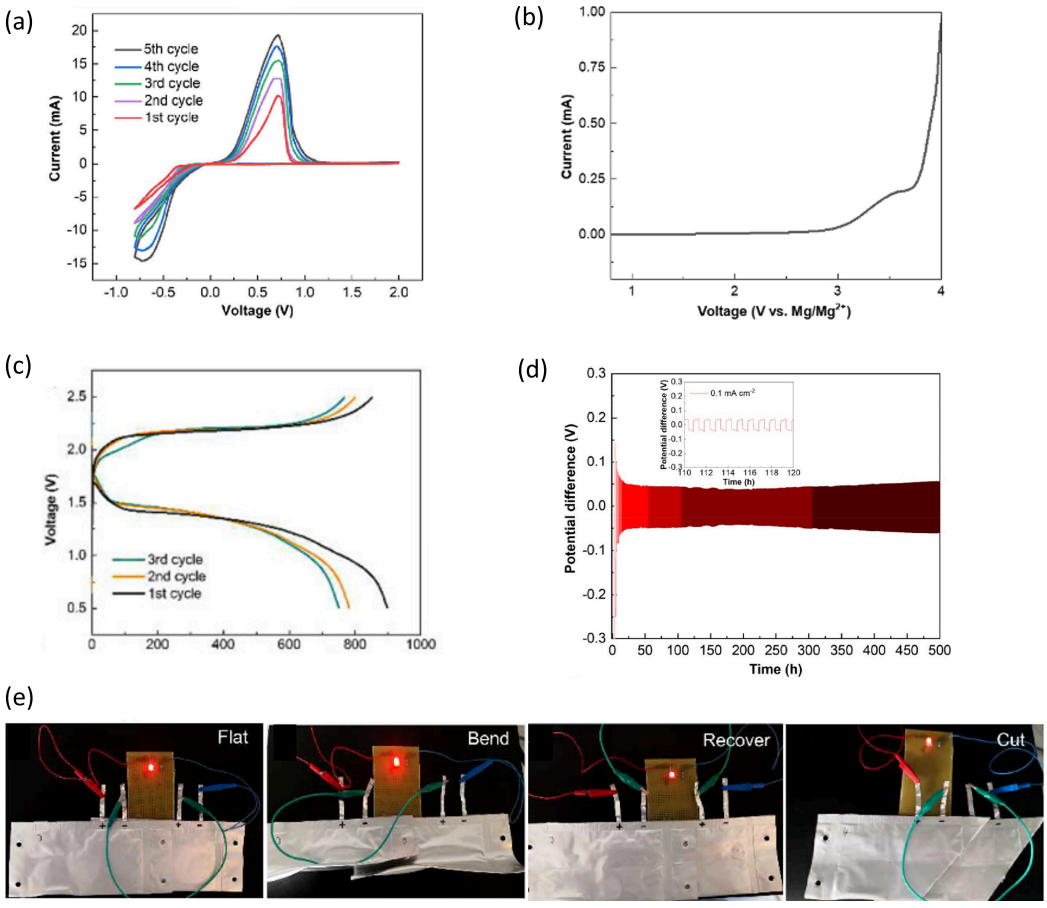

Figure 17. (a) CV curves for Mg plating and stripping using PTHF GPE; (b) LSV of a Mg//SS cell using GPE; (c) Galvanostatic discharge/charge curves of the first three cycles of ACC/S cathode and Mg anode with GPE; (d) Long-term cycling of Mg symmetrical cell with current density of 0.1 mA cm^{-2}; (e) Optical images of LED lamps lighted by pouch cells (Mg//S) under various mechanical deformations.; Reproduced with permission[26]; Copyright © 2022 Elsevier B.V. All rights reserved.

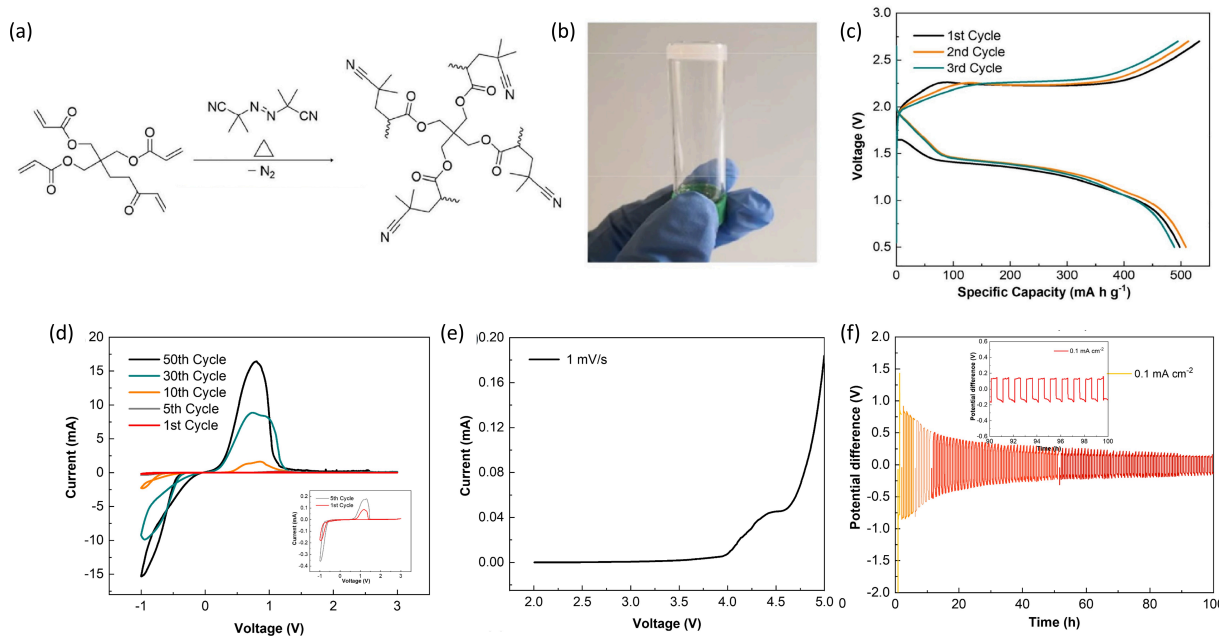

Figure 18. (a) Scheme of the polymerisation of PETEA using AIBN as initiator. (b) Optical image of the formed gel. (c) Galvanostatic discharge/charge curves of the first three cycles of ACC/S cathode and Mg anode with GPE. (d) CV curves for Mg plating and stripping using the PPTEA-based GPE. (e) LSV of a Mg//SS cell using the GPE; (f) Long-term cycling of Mg symmetrical cell with current density of 0.1 mA cm^{-2}.; Reproduced with permission[26]; Copyright © 2022 Elsevier B.V. All rights reserved.

(10^{-6} to 10^{-4} mS cm^{-1} at rt) and especially for the $[B(hfip)_4]^-$-composition, a high anodic stability (5.5 V vs. SS). Unfortunately, they could not observe reversible Mg plating/stripping in this fully solid system.

Recently, Sun *et al.* presented another approach.[105] Using "thiol-ene" click chemistry a polymeric network within a glass fiber separator was produced. First, a magnesium alkoxychloride (GDAEMgCl) was synthesized using glycerol α,α′-diallyl ether (GDAE; 1,3-bis(allyloxy)propan-2-ol) and *n*-butyl magnesium chloride as precursor, and THF as solvent. Removing the THF yielded in a white powder of the desired product. GDAEMgCl (magnesium 1,3-bis(allyloxy)propan-2-olate chloride) was redissolved in THF and $AlCl_3$ was added to form the magnesium complex GDAEAM ($[Mg_2Cl_3][$((1,3-bis(allyloxy)propan-2-yl)oxy)trichloroaluminate). After that 3,6-dioxa-1,8-octanedithiol (DODTH) and the photoinitiator 2,2-dimethoxy-2-phenylacetophenone (DMPA) were added to obtain the final precursor solution. A glass fiber separator was immerged in the precursor solution and then treated with UV light to initiate the polymerization (Figure 19a–c). Subsequently the separator-polymer membrane was rinsed with THF to remove residual starting materials. Finally, the separator-polymer membrane (GPE@GF) was immersed in fresh THF and utilized in a battery, serving as both an electrolyte and a separator. They demonstrated reversible Mg plating/stripping (Figure 19d–e). relatively low polarization (< 200 mV), good Coulombic efficiency (95.2 %) and anodic stability (~3.6 V vs. Mo). They proofed the feasibility of their system in full cells, using Chevrel phase as cathode and magnesium metal as anode at coin cell and small pouch cell level.

Chen *et al.* showed again an *in situ* approach using ring-opening polymerization within the separator.[106] First, two solutions were prepared: a solution of 2,2,6,6-tetramethylpiperidinylmagnesium chloride lithium chloride (TMPL) as Mg ion conducting salt in THF and a solution of aluminum trifluoromethanesulfonate ($Al(OTf)_3$) as initiator in 1,3-dioxolane (DOL). The TMPL solution was added to the initiator solution and after vigorous stirring the resulting precursor solution was injected into the cell and within 24 hours the polymerization of DOL to poly(1,3-dioxolane) took place within the separator as skeleton. With their system they were able to show reversible Mg plating/stripping, low polarization (~100 mV), relatively high Coulombic efficiency (98.9 %), but unfortunately low anodic stability (~2.5 V vs. Al). Furthermore, they presented the applicability in full cells (coin cell and pouch cell level), using Chevrel phase and copper selenide as cathodes and Mg metal as anode.

Both systems, discussed before, contain chloride ions and are using a separator as skeleton, so the approach by Wang *et al.* is a different way with a chloride- and additional separator-free system. Their polymer electrolyte is based on $Mg[B(hfip)_4]_2$.[107] They prepared two solutions: PVDF-HFP was dissolved in DME and $Mg[B(hfip)_4]_2$ in PEGDME (poly(ethylene glycol) dimethyl ether) at a ratio of 30 ethylene oxide units per Mg^{2+} cation. The Mg-salt solution was added to the PVDF-HFP-solution to form a gel-like solution after stirring for 30 min and then casted into a Petri dish.

They solvent was removed at 80 °C, obtaining a free-standing polymer film (Figure 20), which demonstrated reversible Mg plating/stripping, with a polarisation of about 500 mV, for 1000 cycles (Figure 21d). The polarisation was reduced to

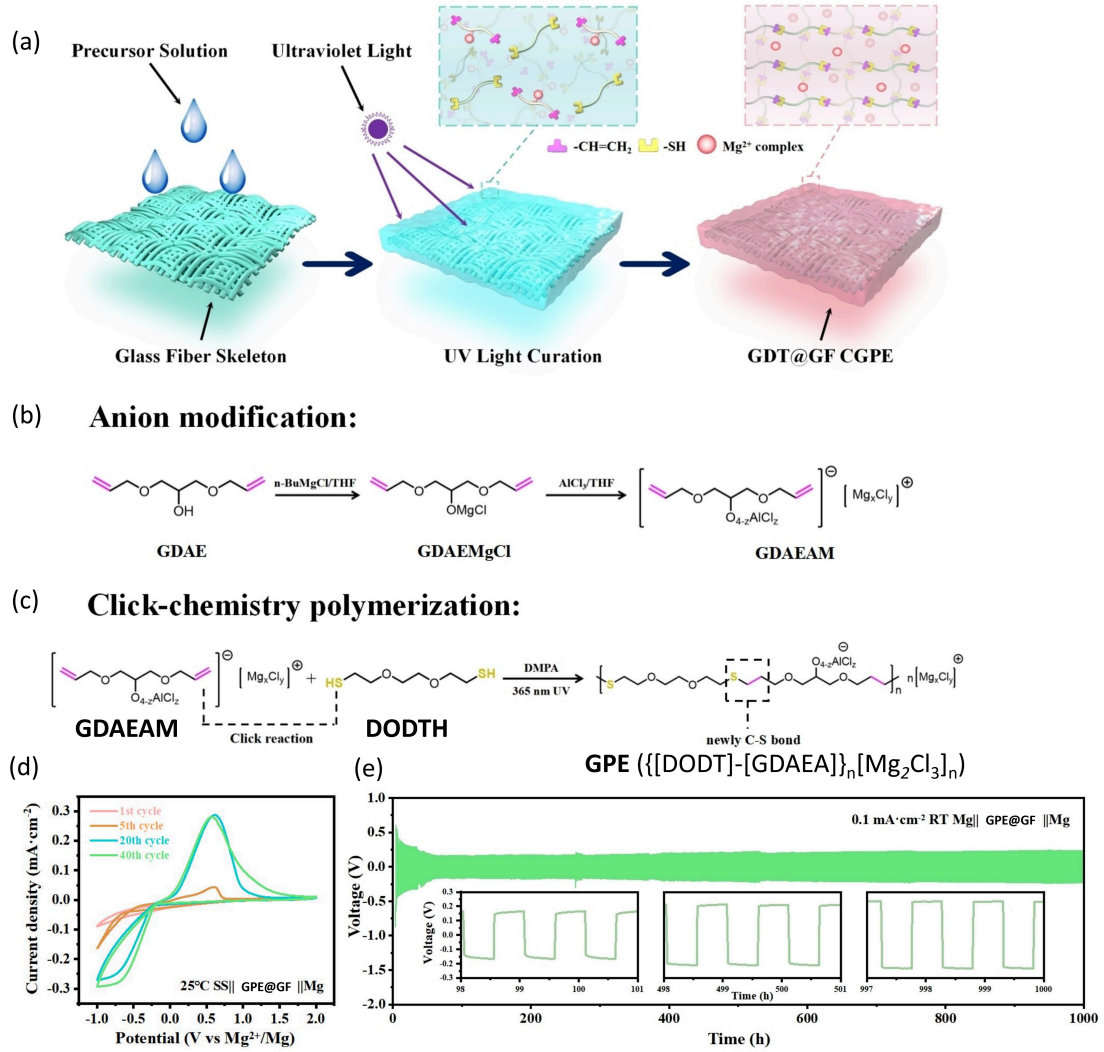

Figure 19. (a) Schematic illustration of the UV light induced polymerization within the glass fiber separator. (b–c) Chemical reaction pathways to the modified anion (b) and the "thiol-ene" polymerisation (c). (d) Cyclic voltammetry curves (Mg//SS) for Mg plating/stripping for GPE@GF (e) Long-term cycling of Mg//Mg cells using GPE@GF. Reproduced with permission,[106] Copyright © 2024 Wiley-VCH GmbH.

approximately 250 mV by soaking the polymer film in a 0.4 M $Mg[B(hfip)_4]_2$/DME solution, which also remained stable for 1000 cycles (Figure 21e). The current response for Mg plating/stripping also increased from 0.03 mA cm^{-2} to 5.0 mA cm^{-2} (Figure 21a–b). Applying the soaked GPE in a Mg//S cell demonstrated an improved performance compared to liquid electrolytes. The cell with GPE maintained a capacity of 200 mAh g^{-1} after 300 cycles, whereas this value was reached already in less than 100 cycles using a liquid electrolyte (Figure 21c). This work once again demonstrates the successful application of a chloride-free system with a self-standing GPE that functions as both an electrolyte and a separator.

The properties of the discussed polymer electrolytes are summarized in Table 4. It has been demonstrated that many parameters, including the salt, the polymer, fillers, plasticizers and the amounts of solvent residues, significantly affect the performance. A deeper investigation in chloride-free systems, especially of the new single salts (e.g. $Mg[B(hfip)_4]_2$), is necessary to identify an optimal system suitable for a broad application.

6. Summary and Perspectives

This review provides a summary of the existing electrolytes used in current research of rechargeable magnesium metal batteries. It summarizes different types of electrolytes, identifies the relevant components, and highlights recent advances in addressing the various challenges posed using magnesium metal as an anode and the appropriate cathode materials. However, achieving a completely fair comparison is often challenging, as the cycle life of Mg metal electrodes—and, ultimately, that of rechargeable magnesium batteries—depends on more than just the electrolyte. Factors such as cell configuration, the thickness of metal anodes, the choice of solvent, applied current density, surface capacity, separator properties, and characteristics of the cathode all significantly

influence the cycle life. Therefore, it is crucial to consider the entire battery system when assessing performance. If we now take into account the following factors to the single salts—conductivity, oxidative stability, molecular weight, ease of synthesis and cathode compatibility—$Mg[B(hfip)_4]_2$ and $Mg[Al(hfip)_4]_2$ show comparable performance. The borate salt shows a slight advantage in terms of molecular weight and synthesis and the aluminate salt performs better regarding conductivity. The carborane salts loose due to their complex synthesis. Based on the discussed developments of batteries with magnesium metal anodes and the various challenges, we propose the following perspectives:

Several new magnesium salts for electrolytes have already been developed. A simple and cost-effective synthetic procedure is apart from the electrochemical performance one key factor regarding costs and commercialization. Furthermore, the development of fluorine-free salts would be important for more sustainability.

To enhance the anode-electrolyte interface and improve long-term stability and reversibility, more detailed investigations into additives are necessary. The combination of a single salt, which is simple to synthesize, and an additive can be a smooth way reaching good performance and easy upscalability.

Addressing the long-time stability of RMBs further investigations should be done in development of suitable solid and/or quasi-solid polymer electrolytes. This type of electrolyte is apart from modified separators one of the possibilities to mitigate the dissolution of the cathode material. Furthermore, it can enhance the safety of the batteries. Especially the combination of the newly developed single salts as polymer electrolyte should be further evaluated.

There is still significant potential to enhance the development of magnesium battery systems to address current challenges. For instance, various types of separators, aside from other cell components, can significantly impact the system's performance. We would like to emphasize again that to ensure successful development for broader applications, it is therefore essential to consider the entire system on the basis of comprehensive full-cell studies.

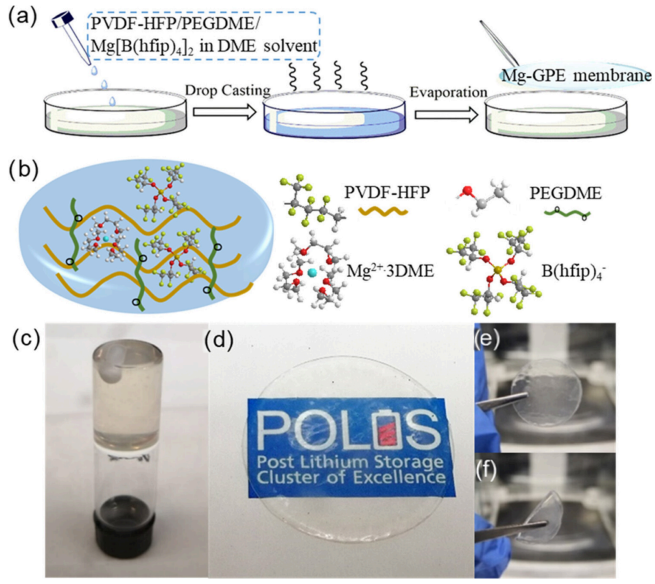

Figure 20. (a) Illustration of the Mg-gel polymer electrolyte (Mg-GPE) membrane preparation. (b) Schematic composition of the Mg-GPE.; Optical images of (c) the prepared gel solution kept overnight in the glovebox, (d) the pristine Mg-GPE membrane, and (e, f) the Mg-GPE disks cut into a specific size.; Reproduced under terms of the CC-BY license,[107] Copyright © 2018 L. Wang, S. Riedel, A. Welle, S. Vincent, S. Dinda, B. Dasari, J. M. Garcia Lastra, B. Esser, Z. Zhao-Karger; Published by American Chemical Society 2024.

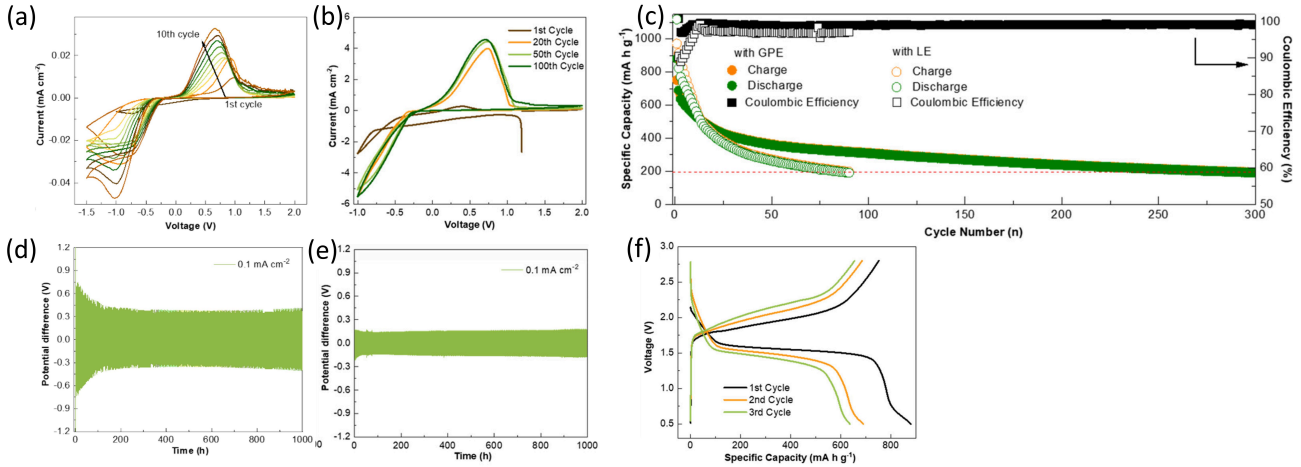

Figure 21. (a–b) Cyclic voltammetry curves (Mg//Al) for Mg plating/stripping in the dry Mg-GPE (a) and soaked Mg-GPE (b) at a sweep rate of 5 $mV\,s^{-1}$. (c) Comparison of cycling performance of Mg//S cells with the soaked Mg-GPE and 0.4 m $Mg[B(hfip)_4]_2 \cdot 3DME$ in DME as liquid electrolyte at 0.1 C. (d–e) Long-term cycling of Mg//Mg cells using dry Mg-GPE (d) and soaked Mg-GPE (e) at a current density of 0.1 $mA\,cm^{-2}$ (0.05 $mA\,h\,cm^{-2}$ Mg is plated and stripped per cycle). (f) Galvanostatic discharge/charge curves of the $Mg//Mg\text{-}GPE_{soaked}//S$ cell for the first three cycles.; Reproduced under terms of the CC-BY license,[107] Copyright © 2018 L. Wang, S. Riedel, A. Welle, S. Vincent, S. Dinda, B. Dasari, J. M. Garcia Lastra, B. Esser, Z. Zhao-Karger; Published by American Chemical Society 2024.

Table 4. List of polymer electrolytes and a summary of their reported compositions and electrochemical properties.

Electrolyte composition	Ionic Conductivity [mS cm^{-1}]	Anodic stability [V]	Reversible Mg plating/ stripping	Efficiency [%]	Ref.
EtMgBr-PEO-THF	0.0126 at ~90 °C	–	√	–	[92]
EtMgBr-PEO-DBE	0.0158 at ~90 °C	–	√	–	[92]
$Mg(TFSI)_2$-PEO-PMA-alkyl carbonates	2.8 at 20 °C	–	√	–	[93]
$Mg(BuEtAlCl_2)_2$-PVDF-HFP-tetraglyme	3.7 at 25 °C	~2.0 vs. Au	√	–	[94]
$Mg(BuEtAlCl_2)_2$-PEO-tetraglyme	–	~2.0 vs. Au	√	–	[94]
$Mg(BuEtAlCl_2)_2$-PVDF-HFP-THF	–	~2.5vs. Au	√	–	[94]
$Mg(ClO_4)_2$-PVDF-HFP-MgO-alkyl carbonates	8.0 at 25 °C	~3.5 vs. SS	√	–	[97]
$Mg(ClO_4)_2$-PVDF-HFP-SiO_2-alkyl carbonates	11.0 at 25 °C	~3.5 vs. SS	√	–	[98]
[PEGDA-STFSIMg]-$Mg(TFSI)_2$-$MgCl_2$-DME	15.0 at rt	–	√	–	[28]
[PEGDA-STFSIMg]-$Mg(HMDS)_2$-$AlCl_3$-THF	4.3 at rt	–	√	–	[28]
$Mg(OTf)_2$- PVDF-HFP-succinonitrile-EMIOTf	4.1 at rt	~4.1 vs. SS	√	–	[99]
[PEGDMA-STFSIMg]-DMSO	~1.0 at rt	–	○	–	[100]
PTHF–$Mg(BH_4)_2$-$MgCl_2$-THF	0.476 at rt	~2.2 vs. SS	√	–	[101]
$Mg(OTf)_2$-PVDF-HFP-alkyl carbonates-Al_2O_3	3.3 at rt	~3.3 vs. SS	○	–	[25]
$Mg(OTf)_2$-PVDF-HFP-alkyl carbonates-$MgAl_2O_4$	4.0 at rt	~3.3 vs. SS	○	–	[25]
FTG–$Mg(BH_4)_2$-$MgCl_2$-THF	0.0451 at rt	4.8 vs. Pt	√	100	[24]
$Mg(NO_3)_2 \cdot 6H_2O$-CA-DMF	0.919 at rt	3.65 vs SS	○	-	[102]
$Mg(TFSI)_2$-PCL-PTMC	~0.1 at 60 °C	–	√	–	[103]
$Mg(TFSI)_2$-PCL-PEO	~0.1 at 60 °C	–	○	–	[103]
$Mg[B(hfip)_4]_2$-$Mg(BH_4)_2$-PTHF-DME	~2.0 at rt	~3.0 vs. SS	√	99	[26]
$Mg[B(hfip)_4]_2$-PPETEA-DME	3.42 at rt	~4.0 vs. SS	√	99	[26]
$Mg(BH_4)_2$-$Li(BH_4)$-PTHF-diglyme	0.22 at 40 °C	~3.5 vs. SS	√	99.8	[104]
$Mg[B(hfip)_4]_2$-P(BEC)	10^{-4} at rt	5.5 vs. SS	○	–	[27]
$Mg(TFSI)_2$-P(BEC)	10^{-6} at rt	3.6 vs. SS	○	–	[27]
$\{[DODT]\text{-}[GDAEA]\}_n[Mg_2Cl_3]_n$	0.119 at rt	3.6 vs. Mo	√	95.2	[105]
TMPL-PDOL–$Al(OTf)_3$-THF	0.28 at rt	~2.5 vs. Al	√	98.9	[106]
$Mg[B(hfip)_4]_2$- PVDF-HFP-PEGDME (dry)	$2.92 \cdot 10^{-2}$ at rt	>4.0 vs. Al	√	>90	[107]

Abbreviations

14PAQ	1,4-Poly anthraquinone
Ag	Silver
AIBN	Azobisisobutyronitrile
Al	Aluminum
APC	All phenyl complex
B	Boron
Bi	Bismut
BMP	2-*tert*-Butyl-4-methyl-phenolate
BMPMC	Magnesium chloride 2-*tert*-butyl-4-methyl-phenolate
Br	Bromine
Bu	Butyl
C	Carbon
CA	Cellulose acetate
CE	Coulombic efficiency
CE	Counter electrode
Chevrel phase	Mo_6S_8
Cl	Chlorine
CV	Cyclic voltammetry
DBE	Di-*n*-butylether
DME	Dimethoxyethane
DMF	Dimethylformamide
DMPA	2,2-Dimethoxy-2-phenylacetophenone
DMSO	Dimethyl sulfoxide
DODT	3,6-Dioxa-1,8-octanedithiolate
DODTH	3,6-Dioxa-1,8-octanedithiol
DOL	1,3-Dioxolane
DTBP	2,6-di-*tert*-butylphenolate
e. g.	*exempli gratia*
EMI	1-Ethyl-3-methylimidazolium
Et	Ethyl
et al.	*et alii*
F	Fluorine
^{F}Ar	3,5-Bis(trifluoro-methyl)phenyl
FTG	Fluorinated tetraethylene glycol
GDAE	Glycerol α,α′-diallyl ether/1,3-bis(allyloxy)propan-2-ol

GDAEA	1,3-Bis(propyloxy)propan-2-yl)oxy)trichloroaluminate
GDAEAM	$[Mg_2Cl_3][((1,3\text{-bis(allyloxy)propan-2-yl)oxy)trichloroaluminate}$
GF	Glass fiber
GPE	Gel polymer electrolyte
H	Hydrogen
hfip	Hexafluoroisopropyloxy-
Hhfip	Hexafluoroisopropanol
HMDS	Bis(trimethylsilyl)amide
H-PFP	Perfluoro pinacol
I	Iodine
In	Indium
MBA	Magnesium bis-(diisopropyl)amide
m-Carborane	*meta*-Carborane
Mg	Magnesium
Mo	Molybdenum
MSS	Metal ion 4-vinylbenzenesulfonate
MSTFSI	Metal ion 4-styrenesulfonyl(trifluoromethane-sulfonyl) imide
N	Nitrogen
Na	Sodium
n-Bu	*n*-Butyl
Ni	Nickel
O	Oxygen
O^FPh	Pentafluorophenolate
O*t*-Bu	*tert*-Butoxy
OTf	Trifluoromethanesulfonate
O*t*-^{F}Bu	Perfluoro-*tert*-butoxy
P(BEC)	Poly(2-butyl-2-ethyltrimethylene-carbonate
PCL-PTMC	Poly(ε-caprolactone-*co*-trimethylene carbonate
PDOL	Poly(1,3-dioxolane)
PEGDA	Poly(ethylene glycol) diacrylate
PEGDMA	Poly(ethylene glycol) dimethacrylate
PEGDME	Polyethylene glycol dimethyl ether
PEO	Polyethylene oxide
PEO-PMA	Poly(ethylene oxide)-modified poly(methacrylate
PETEA	Pentaerythritol tetraacrylate
PFP	Perfluoro-pinacolato
PFTB	Perfluoro-*tert*-butoxy
Ph	Phenyl
PP_{14}	1-Butyl-1-methylpiperidinium
PPETEA	Poly-pentaerythritol tetraacrylate
Pt	Platinum
PTHF	Polytetrahydrofuran
PVDF	Polyvinylidene fluoride
PVDF-HFP	Poly(vinylidene fluoride-*co*-hexafluoropropylene)
RE	Reference electrode
RMB	Rechargeable magnesium battery
S	Sulfur
SEI	Solid electrolyte interface
SEM	Scanning electron microscopy
SHE	Standard hydrogen electrode
SPAN	Sulfurized polyacrylonitrile
SS	Stainless steel
TBA	Tetrabutylammonium
TFSI	Bis(trifluoromethane)sulfonimide
THF	Tetrahydrofuran
TMPL	2,2,6,6-Tetramethylpiperidinylmagnesium chloride lithium chloride
UV	Ultraviolet

Acknowledgements

This work was funded by the German Research Foundation (DFG) under Project ID 390874152 (POLiS Cluster of Excellence). This work contributes to the research performed at CELEST (Center for Electrochemical Energy Storage Ulm-Karlsruhe). Furthermore, we thank Dr. Christian Bäucker (Helmholtz Institute Ulm), especially in creating the crystal structures in Diamond 4.0. and Dr. Sebahat Topal (Helmholtz Institute Ulm) for their support. Open Access funding enabled and organized by Projekt DEAL.

Conflict of Interests

The authors declare no conflict of interest.

Data Availability Statement

The data that support the findings of this study are available from the corresponding author upon reasonable request.

Keywords: Magnesium metal battery · Magnesium electrolyte · Anode-electrolyte interface · Polymer electrolyte

[1] H. D. Yoo, I. Shterenberg, Y. Gofer, G. Gershinsky, N. Pour, D. Aurbach, *Energy Environ. Sci.* **2013**, *6*, 2265.
[2] J. Muldoon, C. B. Bucur, T. Gregory, *Chem. Rev.* **2014**, *114*, 11683–11720.
[3] Q. Wu, K. Shu, L. Sun, H. Wang, *Front. Mater.* **2021**, *7*, 612134.
[4] W. Zhao, Y. Liu, X. Zhao, Z. Pan, J. Chen, S. Zheng, L. Qu, X. Yang, *Chem. Eur. J.* **2023**, *29*, e202203334.
[5] Y. Liang, H. Dong, D. Aurbach, Y. Yao, *Nat. Energy* **2020**, *5*, 646–656.
[6] Z. Zhao-Karger, M. Fichtner, *Front. Chem.* **2019**, *6*, 656.
[7] W. Ren, M. Cheng, Y. Wang, D. Zhang, Y. Yang, J. Yang, J. Wang, Y. NuLi, *Batter Supercaps.* **2022** *5* e202200263.
[8] R. Deivanayagam, B. J. Ingram, R. Shahbazian-Yassar, *Energy Storage Mater.* **2019**, *21*, 136–153.
[9] T. D. Gregory, R. J. Hoffman, R. C. Winterton *J. Electrochem. Soc.* **1990**, *137*, 775–780.
[10] D. Aurbach, Z. Lu, A. Schechter, Y. Gofer, H. G, izbar, R. Turgeman, Y. Cohen, M. Moshkovich, E. Levi, *Nature* **2000**, *407*, 724–727.
[11] J. Muldoon, C. B. Bucur, A. G. Oliver, J. Zajicek, G. D. Allred, W. C. Boggess, *Energy Environ. Sci.* **2013**, *6*, 482–487.
[12] D.-T. Nguyen, A. Y. S. Eng, M.-F. Ng, V. Kumar, Z. Sofer, A. D. Handoko, G. S. Subramanian, Z. W. Seh, *Cell Rep. Phys. Sci.* **2020**, *1*, 100265.
[13] G. Yang, Y. Li, J. Wang, Y. Lum, C. Y. J. Lim, M.-F. Ng, C. Zhang, Z. Chang, Z. Zhang, A. D. Handoko, T. Ghosh, S. Li, Z. Sofer, W. Liu, Y. Yao, Z. W. Seh, *Energy Environ. Sci.* **2024**, *17*, 1141–1152.
[14] L. C. Merrill, J. L. Schaefer, *Langmuir* **2017**, *33*, 9426–9433.
[15] C. A. Nist-Lund, J. T. Herb, C. B. Arnold, *J. Power Sources* **2017**, *362*, 308–314.
[16] S. A. Brown, S. A. Cussen, R. Kennard, S. Marchesini, J. J. Pryke, A. Rae, S. D. Robertson, R. N. Samajdar, A. J. Wain, *Chem. Commun.* **2022**, *58*, 12070–12073.
[17] Z. Zhao-Karger, M. E. Gil Bardaji, O. Fuhr, M. Fichtner, *J. Mater. Chem. A Mater.* **2017**, *5*, 10815–10820.

[18] O. Tutusaus, R. Mohtadi, T. S. Arthur, F. Mizuno, E. G. Nelson, Y. V. Sevryugina, *Angew. Chem. Int. Ed.* **2015**, *54*, 7900–7904.
[19] D. Chinnadurai, Y. Li, C. Zhang, G. Yang, W. Y. Lieu, S. Kumar, Z. Xing, W. Liu, Z. W. Seh, *Nano Lett.* **2023**, *23*, 11233–11242.
[20] Z. Meng, Z. Li, L. Wang, T. Diemant, D. Bosubabu, Y. Tang, R. Berthelot, Z. Zhao-Karger, M. Fichtner, *ACS Appl. Mater. Interfaces* **2021**, *13*, 37044–37051.
[21] Z. Li, T. Diemant, Z. Meng, Y. Xiu, A. Reupert, L. Wang, M. Fichtner, Z. Zhao-Karger, *ACS Appl. Mater. Interfaces* **2021**, *13*, 33123–33132.
[22] R. Horia, D.-T. Nguyen, A. Y. S. Eng, Z. W. Seh, *Nano Lett.* **2021**, *21*, 8220–8228.
[23] S. S. Kim, K. A. See, *ACS Appl. Mater. Interfaces* **2021**, *13*, 671–680.
[24] H. Fan, Y. Zhao, J. Xiao, J. Zhang, M. Wang, Y. Zhang, *Nano Res.* **2020**, *13*, 2749–2754.
[25] J. Sharma, S. Hashmi, *Polym. Compos.* **2019**, *40*, 1295–1306.
[26] L. Wang, Z. Li, Z. Meng, Y. Xiu, B. Dasari, Z. Zhao-Karger, M. Fichtner, *Energy Storage Mater.* **2022**, *48*, 155–163.
[27] D. A. Sundermann, B. Park, V. Hirschberg, J. L. Schaefer, P. Théato, *ACS Omega* **2023**, *8*, 23510–23520.
[28] H. O. Ford, L. C. Merrill, P. He, S. P. Upadhyay, J. L. Schaefer, *Macromolecules* **2018**, *51*, 8629–8636.
[29] O. Mizrahi, N. Amir, E. Pollak, O. Chusid, V. Marks, H. Gottlieb, L. Larush, E. Zinigrad, D. Aurbach, *J. Electrochem. Soc.* **2008**, *155*, A103.
[30] H. S. Kim, T. S. Arthur, G. D. Allred, J. Zajicek, J. G. Newman, A. E. Rodnyansky, A. G. Oliver, W. C. Boggess, J. Muldoon, *Nat. Commun.* **2011**, *2*, 427.
[31] Z. Zhao-Karger, X. Zhao, O. Fuhr, M. Fichtner, *RSC Adv.* **2013**, *3*, 16330.
[32] Z. Zhao-Karger, X. Zhao, D. Wang, T. Diemant, R. J. Behm, M. Fichtner, *Adv. Energy Mater.* **2015**, *5*, 1401155.
[33] F. Wang, Y. Guo, J. Yang, Y. Nuli, S. Hirano, *Chem. Commun.* **2012**, *48*, 10763.
[34] Z. Zhao-Karger, J. E. Mueller, X. Zhao, O. Fuhr, T. Jacob, M. Fichtner, *RSC Adv.* **2014**, *4*, 26924–26927.
[35] J. T. Herb, C. A. Nist-Lund, C. B. Arnold, *J. Mater. Chem. A Mater.* **2017**, *5*, 7801–7805.
[36] J. Long, S. Tan, J. Wang, F. Xiong, L. Cui, Q. An, L. Mai, *Angew. Chem. Int. Ed.* **2023**, *62*, e202301934.
[37] K. Sato, G. Mori, T. Kiyosu, T. Yaji, K. Nakanishi, T. Ohta, K. Okamoto, Y. Orikasa, *Sci. Rep.* **2020**, *10*, 7362.
[38] L. Yang, C. Yang, Y. Chen, Z. Pu, Z. Zhang, Y. Jie, X. Zheng, Y. Xiao, S. Jiao, Q. Li, D. Xu, *ACS Appl. Mater. Interfaces* **2021**, *13*, 30712–30721.
[39] J. Xiao, X. Zhang, H. Fan, Y. Zhao, Y. Su, H. Liu, X. Li, Y. Su, H. Yuan, T. Pan, Q. Lin, L. Pan, Y. Zhang, *Adv. Mater.* **2022**, *34*, 2203783.
[40] B. Pan, J. Zhang, J. Huang, J. T. Vaughey, L. Zhang, S.-D. Han, A. K. Burrell, Z. Zhang, C. Liao, *Chem. Commun.* **2015**, *51*, 6214–6217.
[41] C. Liao, N. Sa, B. Key, A. K. Burrell, L. Cheng, L. A. Curtiss, J. T. Vaughey, J.-J. Woo, L. Hu, B. Pan, Z. Zhang, *J. Mater. Chem. A Mater.* **2015**, *3*, 6082–6087.
[42] B. Pan, J. Huang, N. Sa, S. M. Brombosz, J. T. Vaughey, L. Zhang, A. K. Burrell, Z. Zhang, C. Liao, *J. Electrochem. Soc.* **2016**, *163*, A1672–A1677.
[43] B. Lee, J.-H. Cho, H. R. Seo, S. Bin Na, J. H. Kim, B. W. Cho, T. Yim, S. H. Oh, *J. Mater. Chem. A Mater.* **2018**, *6*, 3126–3133.
[44] D.-T. Nguyen, A. Y. S. Eng, M.-F. Ng, V. Kumar, Z. Sofer, A. D. Handoko, G. S. Subramanian, Z. W. Seh, *Cell Rep. Phys. Sci.* **2020**, *1*, 100265.
[45] W. Ren, D. Wu, *ACS Appl. Mater. Interfaces* **2021**, *13*, 32957–32967.
[46] S. Ilic, S. N. Lavan, N. J. Leon, H. Liu, A. Jain, B. Key, R. S. Assary, C. Liao, J. G. Connell, *ACS Appl. Mater. Interfaces* **2024**, *16*, 435–443.
[47] K. Tang, A. Du, X. Du, S. Dong, C. Lu, Z. Cui, L. Li, G. Ding, F. Chen, X. Zhou, G. Cui, *Small* **2020**, *16*, 10.1002/smll.202005424.
[48] T. J. Carter, R. Mohtadi, T. S. Arthur, F. Mizuno, R. Zhang, S. Shirai, J. W. Kampf, *Angew. Chem. Int. Ed.* **2014**, *53*, 3173–3177.
[49] N. Pour, Y. Gofer, D. T. Major, D. Aurbach, *J. Am. Chem. Soc.* **2011**, *133*, 6270–6278.
[50] B. Pan, J. Zhang, J. Huang, J. T. Vaughey, L. Zhang, S.-D. Han, A. K. Burrell, Z. Zhang, C. Liao, *Chem. Commun.* **2015**, *51*, 6214–6217.
[51] H. Dong, Y. Liang, O. Tutusaus, R. Mohtadi, Y. Zhang, F. Hao, Y. Yao, *Joule* **2019**, *3*, 782–793.
[52] R. Mohtadi, M. Matsui, T. S. Arthur, S. Hwang, *Angew. Chem. Int. Ed.* **2012**, *51*, 9780–9783.
[53] H. Dong, O. Tutusaus, Y. Liang, Y. Zhang, Z. Lebens-Higgins, W. Yang, R. Mohtadi, Y. Yao, *Nat. Energy* **2020**, *5*, 1043–1050.
[54] N. T. Hahn, T. J. Seguin, K.-C. Lau, C. Liao, B. J. Ingram, K. A. Persson, K. R. Zavadil, *J. Am. Chem. Soc.* **2018**, *140*, 11076–11084.
[55] A. W. Tomich, J. Chen, V. Carta, J. Guo, V. Lavallo *ACS Cent. Sci* . **2024**, *10*, 264–271..
[56] M. Nava, I. V. Stoyanova, S. Cummings, E. S. Stoyanov, C. A. Reed, *Angew. Chem. Int. Ed.* **2014**, *53*, 1131–1134.
[57] L. Toom, A. Kütt, I. Leito, *Dalton Transactions* **2019**, *48*, 7499–7502.
[58] V. Lavallo, J. Guo, L. Geng, S. Lee, J. Estrada, S. McArthur, **2018**, US20180175456 A1.
[59] N. Tanaka, Y. Shoji, T. Fukushima, *Organometallics* **2016**, *35*, 2022–2025.
[60] Z. Janoušek, C. L. Hilton, P. J. Schreiber, J. Mich, *Collect. Czech. Chem. Commun.* **2002**, l*67*, 1025–1034.
[61] E. Abouzari-Lotf, R. Azmi, Z. Li, S. Shakouri, Z. Chen, Z. Zhao-Karger, S. Klyatskaya, J. Maibach, M. Ruben, M. Fichtner, *ChemSusChem* **2021**, *14*, 1840–1846.
[62] Y. Xiu, A. Mauri, S. Dinda, Y. Pramudya, Z. Ding, T. Diemant, A. Sarkar, L. Wang, Z. Li, W. Wenzel, M. Fichtner, Z. Zhao-Karger, *Angew. Chem. Int. Ed.* **2023**, *62*, e202212339.
[63] Y. Xiu, Z. Li, V. Bhaghavathi Parambath, Z. Ding, L. Wang, A. Reupert, M. Fichtner, Z. Zhao-Karger, *Batter. Supercaps* **2021**, *4*, 1850–1857.
[64] P. Wang, J. Kappler, B. Sievert, J. Häcker, K. Küster, U. Starke, F. Ziegler, M. R. Buchmeiser, *Electrochim. Acta* **2020**, *361*, 137024.
[65] O. Lužanin, J. Moškon, T. Pavčnik, R. Dominko, J. Bitenc, *Batter. Supercaps* **2023**, *6*, e202200437.
[66] K. Sone, Y. Hayashi, T. Mandai, S. Yagi, Y. Oaki, H. Imai, *J Mater Chem. A Mater.* **2021**, *9*, 6851–6860.
[67] Z. Zhao-Karger, R. Liu, W. Dai, Z. Li, T. Diemant, B. P. Vinayan, C. Bonatto Minella, X. Yu, A. Manthiram, R. J. Behm, M. Ruben, M. Fichtner, *ACS Energy Lett.* **2018**, *3*, 2005–2013.
[68] Z. Li, A. Welle, S. Vincent, L. Wang, S. Fuchs, S. Riedel, A. Roy, D. Bosubabu, J. M. García-Lastra, M. Fichtner, Z. Zhao-Karger, *Adv. Energy Mater* **2023**, *13*, 2302905.
[69] T. Mandai, *ACS Appl. Mater. Interfaces* **2020**, *12*, 39135–39144.
[70] B. Dlugatch, J. Drews, R. Attias, B. Gavriel, A. Ambar, T. Danner, A. Latz, D. Aurbach, *J. Electrochem. Soc.* **2023**, *170*, 090542.
[71] B. Dlugatch, M. Mohankumar, R. Attias, B. M. Krishna, Y. Elias, Y. Gofer, D. Zitoun, D. Aurbach, *ACS Appl. Mater. Interfaces* **2021**, *13*, 54894–54905.
[72] J. Luo, Y. Bi, L. Zhang, X. Zhang, T. L. Liu, *Angew. Chem. Int. Ed.* **2019**, *58*, 6967–6971.
[73] T. Pavčnik, J. Bitenc, K. Pirnat, R. Dominko, *Batter. Supercaps* **2021**, *4*, 815–822.
[74] W. Ren, D. Wu, *ACS Energy Lett.* **2021**, *6*, 3212–3220.
[75] S. Li, J. Zhang, S. Zhang, Q. Liu, H. Cheng, L. Fan, W. Zhang, X. Wang, Q. Wu, Y. Lu, *Nat. Energy* **2024**, *9*, 285–297.
[76] X. Huang, S. Tan, J. Chen, Z. Que, R. Deng, J. Long, F. Xiong, G. Huang, X. Zhou, L. Li, J. Wang, L. Mai, F. Pan, *Adv. Funct. Mater.* **2024**, *34*, 2314146.
[77] J. T. Herb, C. A. Nist-Lund, C. B. Arnold, *ACS Energy Lett.* **2016**, *1*, 1227–1232.
[78] E. N. Keyzer, J. Lee, Z. Liu, A. D. Bond, D. S. Wright, C. P. Grey, *J. Mater. Chem. A Mater.* **2019**, *7*, 2677–2685.
[79] T. Mandai, Y. Youn, Y. Tateyama, *Mater. Adv.* **2021**, *2*, 6283–6296.
[80] T. Pavčnik, J. Imperl, M. Kolar, R. Dominko, J. Bitenc, *J. Mater. Chem. A Mater.* **2024**, *12*, 3386–3397.
[81] T. Pavčnik, M. Lozinšek, K. Pirnat, A. Vizintin, T. Mandai, D. Aurbach, R. Dominko, J. Bitenc, *ACS Appl. Mater. Interfaces* **2022**, *14*, 26766–26774.
[82] Z. Hu, L. Huang, X. Gan, Y. Han, J. Chu, Z. Song, *ACS Appl. Mater. Interfaces* **2024**, *16*, 19014–19025.
[83] S. Bulut, P. Klose, I. Krossing, *Dalton Trans.* **2011**, *40*, 8114.
[84] Y. Filinchuk, B. Richter, T. R. Jensen, V. Dmitriev, D. Chernyshov, H. Hagemann, *Angew. Chem. Int. Ed.* **2011**, *50*, 11162–11166.
[85] X. Li, T. Gao, F. Han, Z. Ma, X. Fan, S. Hou, N. Eidson, W. Li, C. Wang, *Adv. Energy Mater.* **2018**, *8*, 1701728.
[86] S. Hebié, F. Alloin, C. Iojoiu, R. Berthelot, J.-C. Leprêtre, *ACS Appl. Mater. Interfaces* **2018**, *10*, 5527–5533.
[87] S. C. Jung, Y.-K. Han, *J. Phys. Chem. C* **2018**, *122*, 17643–17649.
[88] G. Yang, Y. Li, C. Zhang, J. Wang, Y. Bai, C. Y. J. Lim, M.-F. Ng, Z. Chang, S. Kumar, Z. Sofer, W. Liu, Z. W. Seh, *Nano Lett.* **2022**, *22*, 9138–9146.
[89] X. Mao-Ling, W. Jun, H. Chen-Ji, Z. Lei, K. Hua-Bin, S. Yan-Bin, Y. Hong-Wei, C. Li-Wei, *J. Electrochem.* **2022**, *28*, 2108561.
[90] D.-T. Nguyen, A. Y. S. Eng, R. Horia, Z. Sofer, A. D. Handoko, M.-F. Ng, Z. W. Seh, *Energy Storage Mater.* **2022**, *45*, 1120–1132.
[91] D. Chinnadurai, W. Y. Lieu, S. Kumar, G. Yang, Y. Li, Z. W. Seh, *Nano Lett.* **2023**, *23*, 1564–1572.
[92] C. Liebenow, *Electrochim Acta* **1998**, *43*, 1253–1256.
[93] N. Yoshimoto, S. Yakushiji, M. Ishikawa, M. Morita, *Electrochim. Acta* **2003**, *48*, 2317–2322.

[94] O. Chusid, Y. Gofer, H. Gizbar, Y. Vestfrid, E. Levi, D. Aurbach, I. Riech, *Adv. Mater.* **2003**, *15*, 627–630.
[95] D. Zhou, D. Shanmukaraj, A. Tkacheva, M. Armand, G. Wang, *Chem.* **2019**, *5*, 2326–2352.
[96] D. Zhou, Y. He, R. Liu, M. Liu, H. Du, B. Li, Q. Cai, Q. Yang, F. Kang, *Adv. Energy Mater.* **2015**, *5*, 1500353.
[97] G. P. Pandey, R. C. Agrawal, S. A. Hashmi, *J. Power Sources* **2009**, *190*, 563–572.
[98] G. P. Pandey, R. C. Agrawal, S. A. Hashmi, *J. Solid State Electrochem.* **2011**, *15*, 2253–2264.
[99] J. Sharma, S. A. Hashmi, *Bull. Mater. Sci.* **2018**, *41*, 147.
[100] L. C. Merrill, H. O. Ford, J. L. Schaefer, *ACS Appl. Energy Mater.* **2019**, *2*, 6355–6363.
[101] A. Du, H. Zhang, Z. Zhang, J. Zhao, Z. Cui, Y. Zhao, S. Dong, L. Wang, X. Zhou, G. Cui, *Adv. Mater.* **2019**, *31*, 1805930.
[102] M. Mahalakshmi, S. Selvanayagam, S. Selvasekarapandian, M. V. L. Chandra, P. Sangeetha, R. Manjuladevi, *Ionics (Kiel)* **2020**, *26*, 4553–4565.
[103] B. Park, R. Andersson, S. G. Pate, J. Liu, C. P. O'Brien, G. Hernández, J. Mindemark, J. L. Schaefer, *Energy Mater. Adv.* **2021**, *2021*, 895403.
[104] P. Wang, J. Trück, J. Häcker, A. Schlosser, K. Küster, U. Starke, L. Reinders, M. R. Buchmeiser, *Energy Storage Mater.* **2022**, *49*, 509–517.
[105] Y. Sun, M. Pan, Y. Wang, A. Hu, Q. Zhou, D. Zhang, S. Zhang, Y. Zhao, Y. Wang, S. Chen, M. Zhou, Y. Chen, J. Yang, Nj. Wang, Y. NuLi, *Angew. Chem. Int. Ed.* **2024**, *63*, e202406585.
[106] S. Chen, M. Zhou, D. Zhang, S. Zhang, Y. Zhao, M. Pan, Y. Wang, Y. Sun, J. Yang, J. Wang, *Adv. Funct. Mater.* **2024**, 2408535.
[107] L. Wang, S. Riedel, A. Welle, S. Vincent, S. Dinda, B. Dasari, J. M. Garcia Lastra, B. Esser, Z. Zhao-Karger, *ACS Appl. Energy Mater.* **2024**, *7*, 5857–5868.

Manuscript received: July 21, 2024
Accepted manuscript online: August 22, 2024